Predefined-Time Synchronization of Coupled Competitive Neural Networks

Yanli Huang[1] | Yaxin Gao[1] | Limei Su[1] | Tse Chiu Wong*[2]

[1]Tianjin Key Laboratory of Autonomous Intelligence Technology and Systems, School of Computer Science and Technology, Tiangong University, Tianjin 300387, China
[2]Department of Design Manufacturing and Engineering Management (DMEM), Faculty of Engineering, University of Strathclyde, 75 Montrose Street, Glasgow, Scotland G1 1XJ, UK

Correspondence
*Tse Chiu Wong.
Email: andy.wong@strath.ac.uk

Abstract

The aim of this paper is to study the predefined-time synchronization of coupled competitive neural networks (NNs) as well as the impacts of time-varying delays on the predefined-time synchronization performance. First, the models for drive and response systems of coupled competitive NNs with and without coupling delays are established for the first time in this work. After that, the predefined-time synchronization of the proposed network models is investigated, and some new predefined-time synchronization conditions for the considered drive and response systems are derived by designing novel bilayer controllers and using some inequality techniques. It is worth mentioning that the desired convergence time can be adjusted by presetting the parameters in the controllers in advance. Moreover, the synchronization is achieved in the predefined time regardless of the initial value of the coupled competitive NNs. At last, the proposed synchronization conditions are validated through two examples.

KEYWORDS:
coupled neural networks, predefined-time synchronization, competitive neural networks

1 | INTRODUCTION

In the last few decades, neural networks (NNs) have become an enduring research topic in both theory and practice due to its widespread applications in image processing, optimization, fixed-point computations, associative memory, and so on. Therefore, there is a great number of studies examining the working mechanism of NNs especially their dynamical behaviors [1, 2, 3, 4, 5, 6, 7]. In particular, the fixed/predefined-time synchronization problem of delayed memristive NNs was studied in [6].

In 1983, Cohen and Grossberg [8] first introduced the model of competitive NNs with the purpose of simulating cell inhibition in the field of neurobiology. This class of NN not only describes the slow unsupervised synaptic corrections which is known as long-term memory (LTM), but also represents the fast neural activity which is known as short-term memory (STM). Since competitive NNs have two distinct time scales and can handle information through inhibition, competition, coordination, and excitation between neurons, this class of network has extensive applications in control theory, modern biomedicine and optimization, etc [9, 10, 11]. In consequence, the dynamical behaviors of competitive NNs have evolved as an important topic and some meaningful results on synchronization of competitive NNs have been published [12, 13, 14, 15, 16]. For instances, the authors in [12] obtained several conditions to guarantee the fixed-time and finite-time synchronization of memristor-based competitive NNs with distinct time scales by constructing appropriate controllers. Rajchakit *et al*. [13] analyzed the stability and passivity problems for a class of memristor-based fractional-order competitive NNs by using Caputo's fractional derivation. It is well-known that coupled competitive NNs are formed from a slew of single competitive NNs, each is connecting to others. Nowadays, coupled competitive NNs have received much more attention than the traditional NNs because of their collective dynamics and applications in areas such as secure communication [17, 18]. To cope with the complexity of coupled competitive NNs, the authors in [18] attempted to obtain a series of sufficient conditions in conjunction with new Lyapunov functions and comparison system for achieving synchronization in a finite settling time of coupled competitive NNs.

In the current literature, the synchronization process is mostly examined in infinite time. However, many practical applications are usually supposed to reach synchronization state within finite time [19, 20, 21]. For example, in chaotic secure communication networks, synchronization between the primary and secondary networks is often required in a limited time for security reasons. In 1953, Kamenkov [19] first introduced the definition of finite-time stability. Ahmad *et al*. [20] developed a novel nonlinear finite-time synchronization control algorithm for the multi-switching synchronization between two externally perturbed chaotic systems. The authors in [21] proposed a new finite-time controller that realized multi-switching synchronization of chaotic systems with bounded disturbances using the drive and response system synchronization arrangement. Moreover, some sufficient conditions were derived to ensure that the competitive NNs can realize synchronization in a settling time [22]. However, the settling time of finite-time synchronization relies on the initial state of the drive-response systems. Whereas, obtaining accurate initial values in practical systems is challenging. Thus, to address this challenge, a concept called fixed-time stability was presented. In [23], a new criterion for fixed-time synchronization of competitive NNs was derived to ensure that the settling time is independent of the initial state of the network. Unfortunately, the relationship between settling convergence time and drive-response system's parameters in fixed-time synchronization is normally ambiguous. However, the designer wants to recover the encoded message in any predetermined short enough time during the process of secure communication, so it is essential to develop an innovative control strategy that can realize synchronization within an arbitrary given time, so as to allocate the synchronization's time in advance based on the designer's requirements. In order to achieve this goal, predefined-time stability as depicted by Sánchez-Torres [24] was presented in which the convergence time can be adjusted by tuning parameters. Compared with finite-time synchronization and fixed-time synchronization, predefined-time synchronization has the advantage that the settling time of synchronization does not depend on any initial value and it can be configured as a controller parameter. On this basis, some novel research findings about the predefined-time stability of dynamic systems were obtained [25, 26, 27]. For example, the predefined-time synchronization of competitive NNs was studied in [26]. Unfortunately, the coupling term has not been taken into consideration in their network model. Therefore, there has been no research conducted on predefined-time synchronization for coupled competitive NNs up to now to the best of our knowledge, which motivates the work presented in this paper.

Inspired by the aforementioned research, the objective of this research is to analyze the predefined-time synchronization of coupled competitive NNs with and without time-varying delays. The key findings and main contributions of this work can be summarized as follows. (1) The drive-response network models of coupled competitive NNs encompassing both the case with time-varying delays and the one without time-varying delays are firstly proposed. (2) Different from some existing control method, two novel bilayer predefined-time controllers are designed for two-layer structure of the considered drive and response systems. (3) Several predefined-time synchronization criteria are derived for the proposed coupled competitive NNs respectively. Moreover, the controllers' parameters can be preset to achieve the desired convergence time, enabling synchronization within a predefined time irrespective of the initial values of the coupled competitive NNs. (4) Numerical experiments are conducted to verify the effectiveness of the obtained results.

2 | PRELIMINARIES

2.1 | Notations

Denote $\mathbb{R} = (-\infty, +\infty)$, $\mathbb{R}^n$ is a n-dimensional real vector space, $\mathbb{R}^{n\times m}$ represents the collection of all real $n \times m$ matrices. $\boldsymbol{A}^T$ means the transpose of matrix of $\boldsymbol{A}$. For any vector $\boldsymbol{b}(\lambda) = (b_1(\lambda), b_2(\lambda), \cdots, b_n(\lambda))^T \in \mathbb{R}^n$, let $\|\boldsymbol{b}(\lambda)\| = \sqrt{\sum_{i=1}^n b_i^2(\lambda)}$. $\otimes$ represents the Kronecker product.

2.2 | Network model of single competitive NN

A single competitive NN can be described by the following set of differential equations:

$$\begin{cases} STM: \varepsilon \dot{y}_s(\lambda) = -\varsigma_s y_s(\lambda) + \sum_{j=1}^{n} d_{sj} f_j(y_j(\lambda)) + G_s \sum_{\kappa=1}^{p} w_{s\kappa}(\lambda) v_\kappa, \\ LTM: \dot{w}_{s\kappa}(\lambda) = -\alpha_s w_{s\kappa}(\lambda) + \beta_s v_\kappa f_s(y_s(\lambda)), \end{cases} \tag{1}$$

where $s = 1, 2, \cdots, n$; $y_s(\lambda)$ is current activity level of neuron; $(w_{s1}(\lambda), w_{s2}(\lambda), \cdots, w_{sp}(\lambda))^T$ represents the synaptic vector of neuron, which is going through the external stimulus $\boldsymbol{v} = (v_1, v_2, \cdots, v_p)^T$; $\varsigma_s > 0$ means the self-inhibition rate of neuron; d_{sj} represents the connection weight between neurons; each element in $\boldsymbol{f}(\boldsymbol{y}(\lambda)) = (f_1(y_1(\lambda)), f_2(y_2(\lambda)), \cdots, f_n(y_n(\lambda)))^T$ stands for the activation function; $G_s > 0$ represents the intensity of the external stimulus, ε stands for some time scale in STM; $\alpha_s > 0$ and β_s represent disposable scaling constants. Moreover, the system (1) satisfies the following initial conditions: $f_s(0) \in \mathbb{R}$ and $w_{s\kappa}(0) \in \mathbb{R}$.

Let $\|v\|^2 = v_1^2 + v_2^2 + \cdots + v_p^2$ be a constant and $\theta_s(\lambda) = \sum_{\kappa=1}^{p} w_{s\kappa}(\lambda) v_\kappa$, $s = 1, 2, \cdots, n$. Without loss of generality, let's assume that the input stimulus vector $\boldsymbol{v}$ is normalized to have a magnitude of $\|\boldsymbol{v}\|^2 = 1$. Then, the single competitive NN (1) can be rewritten as:

$$\begin{cases} STM: \varepsilon \dot{y}_s(\lambda) = -\varsigma_s y_s(\lambda) + \sum_{j=1}^{n} d_{sj} f_j(y_j(\lambda)) + G_s \theta_s(\lambda), \\ LTM: \dot{\theta}_s(\lambda) = -\alpha_s \theta_s(\lambda) + \beta_s f_s(y_s(\lambda)). \end{cases} \tag{2}$$

2.3 | Definitions and lemmas

Definition 1. The $\boldsymbol{y}(\lambda) = \boldsymbol{0}$ is referred to be finite-time stable if there is a constant $\lambda^* \geq 0$ satisfying $\boldsymbol{y}(\lambda) = \boldsymbol{0}$ for $\forall \lambda > \lambda^*$, $\forall \boldsymbol{y}(0) \in \mathbb{R}^n$. For $\forall \boldsymbol{y}(0) \in \mathbb{R}^n$, $T(\boldsymbol{y}(0)) = \inf\{\lambda^* : \boldsymbol{y}(\lambda) = 0, \forall \lambda > \lambda^*\}$ is called the settling time function.

Definition 2. The $\boldsymbol{y}(\lambda) = 0$ is called to be fixed-time stable if it is finite-time stable as well as the settling time function $T(\cdot)$ is uniformly bounded, i.e. there exists a scalar $T_{\max} > 0$ such that $T(\boldsymbol{y}(0)) \leq T_{\max}$ for $\forall \boldsymbol{y}(0) \in \mathbb{R}^n$.

Definition 3. The $\boldsymbol{y}(\lambda) = 0$ is called to be predefined-time stable if it is fixed-time stable as well as for $\forall T_c > 0$, $T(\boldsymbol{y}(0)) \leq T_c$ for $\forall \boldsymbol{y}(0) \in \mathbb{R}^n$, where T_c is the predefined time which is not associated with the initial value. In other words, T_c serves as an adjustable parameter in the control design.

Lemma 1. If there is a continuous, radially unbounded Lyapunov function $W(\lambda)$ which meets

$$\dot{W}(\lambda) \leq -\frac{\pi}{\sigma T_c}(W^{1+(\sigma/2)}(\lambda) + W^{1-(\sigma/2)}(\lambda)),$$

in which $T_c > 0$ is a predefined-time constant given in advance and $\sigma \in (0, 1)$ is a real constant. Then, the origin of the error system exhibits global stability within the predefined-time T_c.

Lemma 2. If $a_1, a_2, \cdots, a_n \geq 0$, $0 < \gamma_1 \leq 1$, $\gamma_2 > 1$, then

$$\sum_{\iota=1}^{n} a_\iota^{\gamma_1} \geq \left(\sum_{\iota=1}^{n} a_\iota\right)^{\gamma_1}, \sum_{\iota=1}^{n} a_\iota^{\gamma_2} \geq n^{1-\gamma_2} \left(\sum_{\iota=1}^{n} a_\iota\right)^{\gamma_2}.$$

Lemma 3. For any vectors $\boldsymbol{\alpha}, \boldsymbol{\beta} \in \mathbb{R}^n$ and $n \times n$ square matrix $\boldsymbol{G} > 0$, the following matrix inequality holds:

$$2\boldsymbol{\alpha}^T \boldsymbol{\beta} \leq \boldsymbol{\alpha}^T \boldsymbol{G} \boldsymbol{\alpha} + \boldsymbol{\beta}^T \boldsymbol{G}^{-1} \boldsymbol{\beta}.$$

3 | PREDEFINED-TIME SYNCHRONIZATION OF COUPLED COMPETITIVE NNS

This section considers the following coupled competitive NNs consisting of M single competitive NNs (2) under the assumption of $\varepsilon = 1$:

$$\begin{cases} STM: \dot{\boldsymbol{y}}_\iota(\lambda) = -\boldsymbol{C}\boldsymbol{y}_\iota(\lambda) + \boldsymbol{D}\boldsymbol{f}(\boldsymbol{y}_\iota(\lambda)) + \boldsymbol{G}\boldsymbol{\theta}_\iota(\lambda) + \rho\sum_{i=1}^{M} Q_{\iota i}\boldsymbol{W}\boldsymbol{y}_i(\lambda), \\ LTM: \dot{\boldsymbol{\theta}}_\iota(\lambda) = -\boldsymbol{A}\boldsymbol{\theta}_\iota(\lambda) + \boldsymbol{B}\boldsymbol{f}(\boldsymbol{y}_\iota(\lambda)) + \varrho\sum_{i=1}^{M} H_{\iota i}\boldsymbol{\Gamma}\boldsymbol{\theta}_i(\lambda), \end{cases} \tag{3}$$

where $\iota = 1, 2, \cdots, M$; $\boldsymbol{C} = \text{diag}\,(\varsigma_1, \varsigma_2, \cdots, \varsigma_n)$; $\boldsymbol{D} = (d_{sj})_{n\times n} \in \mathbb{R}^{n\times n}$ is a constant matrix; $\boldsymbol{y}_\iota(\lambda) = (y_{\iota 1}(\lambda), y_{\iota 2}(\lambda), \cdots, y_{\iota n}(\lambda))^T \in \mathbb{R}^n$; $\boldsymbol{f}(\boldsymbol{y}_\iota(\lambda)) = (f_1(y_{\iota 1}(\lambda)), f_2(y_{\iota 2}(\lambda)), \cdots, f_n(y_{\iota n}(\lambda)))^T$; $\boldsymbol{G} = \text{diag}\,(G_1, G_2, \cdots, G_n)$; $\boldsymbol{\theta}_\iota(\lambda) = (\boldsymbol{\theta}_{\iota 1}(\lambda), \boldsymbol{\theta}_{\iota 2}(\lambda), \cdots, \boldsymbol{\theta}_{\iota n}(\lambda))^T$; $\boldsymbol{A} = \text{diag}\,(\alpha_1, \alpha_2, \cdots, \alpha_n)$; $\boldsymbol{B} = \text{diag}(\beta_1, \beta_2, \cdots, \beta_n)$; the positive constants ρ and ϱ mean the overall coupling strengths; $\boldsymbol{W} \in \mathbb{R}^{n\times n} > 0$ and $\boldsymbol{\Gamma} \in \mathbb{R}^{n\times n} > 0$ represent the inner coupling matrix. The coupling configuration matrices $\boldsymbol{Q} = (Q_{\iota i})_{M\times M}$ and $\boldsymbol{H} = (H_{\iota i})_{M\times M}$ have the following definitions:

$$\begin{cases} Q_{\iota i} = Q_{i\iota} > 0, & \text{if there exists a connection between node } \iota \text{ and node } i (\iota \neq i), \\ Q_{\iota i} = Q_{i\iota} = 0, & \text{otherwise } (\iota \neq i), \\ Q_{\iota\iota} = -\sum_{\substack{i=1 \\ i\neq\iota}}^{M} Q_{\iota i}, \iota = 1, 2, \cdots, M, \end{cases}$$

$$\begin{cases} H_{\iota i} = H_{i\iota} > 0, & \text{if node } \iota \text{ and node } i(\iota \neq i) \text{are connected}, \\ H_{\iota i} = H_{i\iota} = 0, & \text{otherwise } (\iota \neq i), \\ H_{\iota\iota} = -\sum_{\substack{i=1 \\ i\neq\iota}}^{M} H_{\iota i}, \iota = 1, 2, \cdots, M. \end{cases}$$

Assumption 1. Throughout this paper, it is assumed that the nonlinear function $f_o(\cdot)(o = 1, 2, \cdots, n)$ satisfies the Lipschitz condition. Namely, there is a positive constant ϖ_o such that

$$|f_o(r_1) - f_o(r_2)| \leq \varpi_o |r_1 - r_2|$$

for any $r_1, r_2 \in \mathbb{R}$. For convenience, denote $\boldsymbol{\Psi} = \text{diag}(\varpi_1^2, \varpi_2^2, \cdots, \varpi_n^2) \in \mathbb{R}^{n\times n}$.

If the coupled competitive NNs (3) is considered as drive system, then the construction of the corresponding response system is achieved as follows:

$$\begin{cases} STM: \dot{\boldsymbol{z}}_\iota(\lambda) = -\boldsymbol{C}\boldsymbol{z}_\iota(\lambda) + \boldsymbol{D}\boldsymbol{f}(\boldsymbol{z}_\iota(\lambda)) + \rho\sum_{i=1}^{M} Q_{\iota i}\boldsymbol{W}\boldsymbol{z}_i(\lambda) + \boldsymbol{G}\boldsymbol{\delta}_\iota(\lambda) + \boldsymbol{u}_\iota(\lambda), \\ LTM: \dot{\boldsymbol{\delta}}_\iota(\lambda) = -\boldsymbol{A}\boldsymbol{\delta}_\iota(\lambda) + \boldsymbol{B}\boldsymbol{f}(\boldsymbol{z}_\iota(\lambda)) + \varrho\sum_{i=1}^{M} H_{\iota i}\boldsymbol{\Gamma}\boldsymbol{\delta}_i(\lambda) + \boldsymbol{m}_\iota(\lambda), \end{cases} \tag{4}$$

where $\iota = 1, 2, \cdots, M$; $\boldsymbol{z}_\iota(\lambda) = (z_{\iota 1}(\lambda), z_{\iota 2}(\lambda), \cdots, z_{\iota n}(\lambda))^T \in \mathbb{R}^n$; $\boldsymbol{f}(\boldsymbol{z}_\iota(\lambda)) = (f_1(z_{\iota 1}(\lambda)), f_2(z_{\iota 2}(\lambda)), \cdots, f_n(z_{\iota n}(\lambda)))^T \in \mathbb{R}^n$; $\boldsymbol{\delta}_\iota(\lambda) = (\boldsymbol{\delta}_{\iota 1}(\lambda), \boldsymbol{\delta}_{\iota 2}(\lambda), \cdots, \boldsymbol{\delta}_{\iota n}(\lambda))^T$, $\boldsymbol{u}_\iota(\lambda) = (u_{\iota 1}(\lambda), u_{\iota 2}(\lambda), \cdots, u_{\iota n}(\lambda))^T \in \mathbb{R}^n$ and $\boldsymbol{m}_\iota(\lambda) = (m_{\iota 1}(\lambda), m_{\iota 2}(\lambda), \cdots, m_{\iota n}(\lambda))^T \in \mathbb{R}^n$ are the controllers to be designed; $\boldsymbol{C}$, $\boldsymbol{A}$, $\boldsymbol{B}$, $\boldsymbol{D}$, $\boldsymbol{G}$, ϱ, ρ, $H_{\iota i}$, $\boldsymbol{\Gamma}$, $Q_{\iota i}$ and $\boldsymbol{W}$ have the same definitions as in system (3).

Let us define error system $\boldsymbol{e}_\iota(\lambda) = \boldsymbol{z}_\iota(\lambda) - \boldsymbol{y}_\iota(\lambda)$ and $\hat{\boldsymbol{e}}_\iota(\lambda) = \boldsymbol{\delta}_\iota(\lambda) - \boldsymbol{\theta}_\iota(\lambda)$. Then

$$\begin{cases} \dot{\boldsymbol{e}}_\iota(\lambda) = -\boldsymbol{C}\boldsymbol{e}_\iota(\lambda) + \boldsymbol{D}[\boldsymbol{f}(\boldsymbol{z}_\iota(\lambda)) - \boldsymbol{f}(\boldsymbol{y}_\iota(\lambda))] + \boldsymbol{G}\hat{\boldsymbol{e}}_\iota(\lambda) + \rho\sum_{i=1}^{M} Q_{\iota i}\boldsymbol{W}\boldsymbol{e}_i(\lambda) + \boldsymbol{u}_\iota(\lambda), \\ \dot{\hat{\boldsymbol{e}}}_\iota(\lambda) = -\boldsymbol{A}\hat{\boldsymbol{e}}_\iota(\lambda) + \boldsymbol{B}[\boldsymbol{f}(\boldsymbol{z}_\iota(\lambda)) - \boldsymbol{f}(\boldsymbol{y}_\iota(\lambda))] + \boldsymbol{m}_\iota(\lambda) + \varrho\sum_{i=1}^{M} H_{\iota i}\boldsymbol{\Gamma}\hat{\boldsymbol{e}}_i(\lambda), \end{cases} \tag{5}$$

where $\boldsymbol{e}_\iota(\lambda) = (e_{\iota 1}(\lambda), e_{\iota 2}(\lambda), \cdots, e_{\iota n}(\lambda))^T$, $\hat{\boldsymbol{e}}_\iota(\lambda) = (\hat{e}_{\iota 1}(\lambda), \hat{e}_{\iota 2}(\lambda), \cdots, \hat{e}_{\iota n}(\lambda))^T$.

The controllers in network (4) are selected as

$$\begin{cases} \boldsymbol{u}_\imath(\lambda) = -c_1\boldsymbol{X}^{\frac{\gamma_1}{2}}\mathbf{sign}(\boldsymbol{e}_\imath(\lambda))|\boldsymbol{e}_\imath(\lambda)|^{1+\gamma_1} - \boldsymbol{V}_\imath\boldsymbol{e}_\imath(\lambda) - c_2\boldsymbol{X}^{-\frac{\gamma_1}{2}}\mathbf{sign}(\boldsymbol{e}_\imath(\lambda))|\boldsymbol{e}_\imath(\lambda)|^{1-\gamma_1}, \\ \boldsymbol{m}_\imath(\lambda) = -c_1\boldsymbol{X}^{\frac{\gamma_1}{2}}\mathbf{sign}(\hat{\boldsymbol{e}}_\imath(\lambda))|\hat{\boldsymbol{e}}_\imath(\lambda)|^{1+\gamma_1} - \boldsymbol{V}_\imath\hat{\boldsymbol{e}}_\imath(\lambda) - c_2\boldsymbol{X}^{-\frac{\gamma_1}{2}}\mathbf{sign}(\hat{\boldsymbol{e}}_\imath(\lambda))|\hat{\boldsymbol{e}}_\imath(\lambda)|^{1-\gamma_1}, \end{cases} \tag{6}$$

where $\boldsymbol{V}_\imath \in \mathbb{R}^{n\times n}$, $0 < \gamma_1 < 1$, $c_1 = \frac{\pi(nM)^{\frac{\gamma_1}{2}}}{2^{\frac{2-\gamma_1}{2}}\gamma_1 T_c}$, $c_2 = \frac{\pi}{2\gamma_1 T_c}$, $\mathbf{sign}(\boldsymbol{e}_\imath(\lambda)) = \mathrm{diag}\,(\mathrm{sign}(e_{\imath1}(\lambda)), \mathrm{sign}(e_{\imath2}(\lambda)), \cdots, \mathrm{sign}(e_{\imath n}(\lambda)))$, $|\boldsymbol{e}_\imath(\lambda)|^{1+\gamma_1} = (|e_{\imath1}(\lambda)|^{1+\gamma_1}, |e_{\imath2}(\lambda)|^{1+\gamma_1}, \cdots, |e_{\imath n}(\lambda)|^{1+\gamma_1})^T$, $|\boldsymbol{e}_\imath(\lambda)|^{1-\gamma_1} = (|e_{\imath1}(\lambda)|^{1-\gamma_1}, |e_{\imath2}(\lambda)|^{1-\gamma_1}, \cdots, |e_{\imath n}(\lambda)|^{1-\gamma_1})^T$, $\mathbf{sign}(\hat{\boldsymbol{e}}_\imath(\lambda)) = \mathrm{diag}\,(\mathrm{sign}(\hat{e}_{\imath1}(\lambda)), \mathrm{sign}(\hat{e}_{\imath2}(\lambda)), \cdots, \mathrm{sign}(\hat{e}_{\imath n}(\lambda)))$, $|\hat{\boldsymbol{e}}_\imath(\lambda)|^{1+\gamma_1} = (|\hat{e}_{\imath1}(\lambda)|^{1+\gamma_1}, |\hat{e}_{\imath2}(\lambda)|^{1+\gamma_1}, \cdots, |\hat{e}_{\imath n}(\lambda)|^{1+\gamma_1})^T$, $|\hat{\boldsymbol{e}}_\imath(\lambda)|^{1-\gamma_1} = (|\hat{e}_{\imath1}(\lambda)|^{1-\gamma_1}, |\hat{e}_{\imath2}(\lambda)|^{1-\gamma_1}, \cdots, |\hat{e}_{\imath n}(\lambda)|^{1-\gamma_1})^T$, $0 < \boldsymbol{X} = \mathrm{diag}\,(X_1, X_2, \cdots, X_n) \in \mathbb{R}^{n\times n}$, $\boldsymbol{X}^{\frac{\gamma_1}{2}} = \mathrm{diag}(X_1^{\frac{\gamma_1}{2}}, X_2^{\frac{\gamma_1}{2}}, \cdots, X_n^{\frac{\gamma_1}{2}})$, $\boldsymbol{X}^{-\frac{\gamma_1}{2}} = \mathrm{diag}(X_1^{-\frac{\gamma_1}{2}}, X_2^{-\frac{\gamma_1}{2}}, \cdots, X_n^{-\frac{\gamma_1}{2}})$.

Remark 1. In the most existing works on NNs, there is only one type of state variables of the neurons. In 1983, a class of competitive NNs was first introduced [8]. Afterwards, Meyer-Bäse *et al*. [9] extended the previous model into two distinct time scales on competitive NNs which usually are composed of two types of state variables including STM and LTM, where STM reflects rapidly changing dynamics of neurons while LTM represents slow activities of unsupervised synaptic modifications. Because competitive NNs have two different time scales and can handle information through inhibition, competition, coordination, and excitation between neurons, this class of network has great application value in image processing, modern biomedicine, optimization and especially secure communication. For example, the encrypted signals should be decrypted within an arbitrary short enough time regardless of the initial values of the systems during the process of secure communication. However, the theories of traditional and finite/fixed-time synchronization cannot solve the above-mentioned problem. Fortunately, predefined-time synchronization overcome this difficulty perfectly which can adjust the convergence time in advance according to the designer's requirements by tuning controller's parameters. Moreover, coupled competitive NNs comprise of multiple interconnected single competitive NNs, and their intricate dynamic behaviors have attracted considerable interest [17, 18]. However, the current studies about coupled competitive NNs mainly focus on traditional synchronization or finite/fixed-time stability. Although the predefined-time synchronization of competitive NNs was investigated in [26], the coupling term has not been taken into consideration in their network model, which inspires the work presented in this paper. To the best of our knowledge, this is the first study to investigate predefined-time synchronization of coupled competitive NNs.

Theorem 1. The network (5) achieves predefined-time synchronization under the action of the bilayer controllers (6) if there exist two matrices $0 < \boldsymbol{X} = \mathrm{diag}(X_1, X_2, \cdots, X_n) \in \mathbb{R}^{n\times n}$ and $\boldsymbol{V} = \mathrm{diag}(\boldsymbol{V}_1, \boldsymbol{V}_2, \cdots, \boldsymbol{V}_M) \in \mathbb{R}^{nM\times nM}$ such that

$$\begin{cases} \boldsymbol{I_M} \otimes \boldsymbol{\Upsilon}_1 - (\boldsymbol{I_M} \otimes \boldsymbol{X})\boldsymbol{V} - \boldsymbol{V}^T(\boldsymbol{I_M} \otimes \boldsymbol{X}) + \rho\boldsymbol{Q} \otimes (\boldsymbol{XW} + \boldsymbol{W}^T\boldsymbol{X}) < 0, \\ \boldsymbol{I_M} \otimes \boldsymbol{\Upsilon}_2 - (\boldsymbol{I_M} \otimes \boldsymbol{X})\boldsymbol{V} - \boldsymbol{V}^T(\boldsymbol{I_M} \otimes \boldsymbol{X}) + \varrho\boldsymbol{H} \otimes (\boldsymbol{X\Gamma} + \boldsymbol{\Gamma}^T\boldsymbol{X}) < 0, \end{cases} \tag{7}$$

where $\boldsymbol{\Upsilon}_1 = -2\boldsymbol{XC} + \boldsymbol{XDD}^T\boldsymbol{X} + 2\boldsymbol{\Psi} + \boldsymbol{XG}$, $\boldsymbol{\Upsilon}_2 = -2\boldsymbol{XA} + \boldsymbol{XBB}^T\boldsymbol{X} + \boldsymbol{XG}$.

Proof. For system (5), construct the following Lyapunov functional

$$P(\lambda) = P_1(\lambda) + P_2(\lambda),$$

where

$$P_1(\lambda) = \sum_{\imath=1}^{M} \boldsymbol{e}_\imath^T(\lambda)\boldsymbol{X}\boldsymbol{e}_\imath(\lambda), \quad P_2(\lambda) = \sum_{\imath=1}^{M} \hat{\boldsymbol{e}}_\imath(\lambda)\boldsymbol{X}\hat{\boldsymbol{e}}_\imath(\lambda).$$

Therefore, it can be stated that

$$\begin{aligned} \dot{P}(\lambda) =& 2\sum_{\imath=1}^{M} \boldsymbol{e}_\imath^T(\lambda)\boldsymbol{X}\dot{\boldsymbol{e}}_\imath(\lambda) + 2\sum_{\imath=1}^{M} \hat{\boldsymbol{e}}_\imath^T(\lambda)\boldsymbol{X}\dot{\hat{\boldsymbol{e}}}_\imath(\lambda) \\ =& 2\sum_{\imath=1}^{M} \boldsymbol{e}_\imath^T(\lambda)\boldsymbol{X}\big[-\boldsymbol{C}\boldsymbol{e}_\imath(\lambda) + \boldsymbol{D}\boldsymbol{f}(\boldsymbol{z}_\imath(\lambda)) - \boldsymbol{D}\boldsymbol{f}(\boldsymbol{y}_\imath(\lambda)) \\ &+ \rho\sum_{i=1}^{M} Q_{\imath i}\boldsymbol{W}\boldsymbol{e}_i(\lambda) - c_1\boldsymbol{X}^{\frac{\gamma_1}{2}}\mathbf{sign}(\boldsymbol{e}_\imath(\lambda))|\boldsymbol{e}_\imath(\lambda)|^{1+\gamma_1} \\ &- c_2\boldsymbol{X}^{-\frac{\gamma_1}{2}}\mathbf{sign}(\boldsymbol{e}_\imath(\lambda))|\boldsymbol{e}_\imath(\lambda)|^{1-\gamma_1} - \boldsymbol{V}_\imath\boldsymbol{e}_\imath(\lambda) + \boldsymbol{G}\hat{\boldsymbol{e}}_\imath(\lambda)\big] \end{aligned}$$

$$
\begin{aligned}
&+2\sum_{\imath=1}^{M}\hat{\boldsymbol{e}}_{\imath}^{T}(\lambda)\boldsymbol{X}\big[-\boldsymbol{A}\hat{\boldsymbol{e}}_{\imath}(\lambda)+\boldsymbol{B}(\boldsymbol{f}(\boldsymbol{z}_{\imath}(\lambda))-\boldsymbol{f}(\boldsymbol{y}_{\imath}(\lambda)))\\
&+\varrho\sum_{i=1}^{M}H_{\imath i}\boldsymbol{\Gamma}\hat{\boldsymbol{e}}_{i}(\lambda)-c_{1}\boldsymbol{X}^{\frac{\gamma_{1}}{2}}\mathbf{sign}(\hat{\boldsymbol{e}}_{\imath}(\lambda))|\hat{\boldsymbol{e}}_{\imath}(\lambda)|^{1+\gamma_{1}}\\
&-c_{2}\boldsymbol{X}^{-\frac{\gamma_{1}}{2}}\mathbf{sign}(\hat{\boldsymbol{e}}_{\imath}(\lambda))|\hat{\boldsymbol{e}}_{\imath}(\lambda)|^{1-\gamma_{1}}-\boldsymbol{V}_{\imath}\hat{\boldsymbol{e}}_{\imath}(\lambda)\big].
\end{aligned}
\tag{8}
$$

Obviously,

$$
2\boldsymbol{e}_{\imath}^{T}(\lambda)\boldsymbol{X}\boldsymbol{D}(\boldsymbol{f}(\boldsymbol{z}_{\imath}(\lambda))-\boldsymbol{f}(\boldsymbol{y}_{\imath}(\lambda)))\leq\boldsymbol{e}_{\imath}^{T}(\lambda)(\boldsymbol{X}\boldsymbol{D}\boldsymbol{D}^{T}\boldsymbol{X}+\boldsymbol{\Psi})\boldsymbol{e}_{\imath}(\lambda),
\tag{9}
$$

$$
2\hat{\boldsymbol{e}}_{\imath}^{T}(\lambda)\boldsymbol{X}\boldsymbol{B}(\boldsymbol{f}(\boldsymbol{z}_{\imath}(\lambda))-\boldsymbol{f}(\boldsymbol{y}_{\imath}(\lambda)))\leq\hat{\boldsymbol{e}}_{\imath}^{T}(\lambda)\boldsymbol{X}\boldsymbol{B}\boldsymbol{B}^{T}\boldsymbol{X}\hat{\boldsymbol{e}}_{\imath}(\lambda)+\boldsymbol{e}_{\imath}^{T}(\lambda)\boldsymbol{\Psi}\boldsymbol{e}_{\imath}(\lambda).
\tag{10}
$$

In addition,

$$
\begin{aligned}
2\sum_{\imath=1}^{M}\boldsymbol{e}_{\imath}^{T}(\lambda)\boldsymbol{X}\boldsymbol{G}\hat{\boldsymbol{e}}_{\imath}(\lambda)\leq&2\sum_{\imath=1}^{M}\sum_{s=1}^{n}|e_{\imath s}(\lambda)|X_{s}G_{s}|\hat{e}_{\imath s}(\lambda)|\\
\leq&\sum_{\imath=1}^{M}\sum_{s=1}^{n}X_{s}G_{s}(e_{\imath s}^{2}(\lambda)+\hat{e}_{\imath s}^{2}(\lambda))\\
=&\sum_{\imath=1}^{M}\sum_{s=1}^{n}X_{s}G_{s}e_{\imath s}^{2}(\lambda)+\sum_{\imath=1}^{M}\sum_{s=1}^{n}X_{s}G_{s}\hat{e}_{\imath s}^{2}(\lambda)\\
=&\sum_{\imath=1}^{M}\boldsymbol{e}_{\imath}^{T}(\lambda)\boldsymbol{X}\boldsymbol{G}\boldsymbol{e}_{\imath}(\lambda)+\sum_{\imath=1}^{M}\hat{\boldsymbol{e}}_{\imath}^{T}(\lambda)\boldsymbol{X}\boldsymbol{G}\hat{\boldsymbol{e}}_{\imath}(\lambda).
\end{aligned}
\tag{11}
$$

From Lemma 2, one has

$$
\begin{aligned}
2c_{1}\sum_{\imath=1}^{M}\boldsymbol{e}_{\imath}^{T}(\lambda)\boldsymbol{X}^{\frac{2+\gamma_{1}}{2}}\mathbf{sign}(\boldsymbol{e}_{\imath}(\lambda))|\boldsymbol{e}_{\imath}(\lambda)|^{1+\gamma_{1}}=&2c_{1}\sum_{\imath=1}^{M}\sum_{s=1}^{n}X_{s}^{\frac{2+\gamma_{1}}{2}}|e_{\imath s}(\lambda)|^{2+\gamma_{1}}\\
\geq&2\frac{c_{1}}{n^{\frac{\gamma_{1}}{2}}}\sum_{\imath=1}^{M}\left(\sum_{s=1}^{n}X_{s}e_{\imath s}^{2}(\lambda)\right)^{\frac{2+\gamma_{1}}{2}}\\
=&2\frac{c_{1}}{n^{\frac{\gamma_{1}}{2}}}\sum_{\imath=1}^{M}\left(\boldsymbol{e}_{\imath}^{T}(\lambda)\boldsymbol{X}\boldsymbol{e}_{\imath}(\lambda)\right)^{\frac{2+\gamma_{1}}{2}}.
\end{aligned}
\tag{12}
$$

$$
\begin{aligned}
2c_{2}\sum_{\imath=1}^{M}\boldsymbol{e}_{\imath}^{T}(\lambda)\boldsymbol{X}^{\frac{2-\gamma_{1}}{2}}\mathbf{sign}(\boldsymbol{e}_{\imath}(\lambda))|\boldsymbol{e}_{\imath}(\lambda)|^{1-\gamma_{1}}=&2c_{2}\sum_{\imath=1}^{M}\sum_{s=1}^{n}X_{s}^{\frac{2-\gamma_{1}}{2}}|e_{\imath s}(\lambda)|^{2-\gamma_{1}}\\
\geq&2c_{2}\sum_{\imath=1}^{M}\left(\sum_{s=1}^{n}X_{s}e_{\imath s}^{2}(\lambda)\right)^{\frac{2-\gamma_{1}}{2}}\\
=&2c_{2}\sum_{\imath=1}^{M}(\boldsymbol{e}_{\imath}^{T}(\lambda)\boldsymbol{X}\boldsymbol{e}_{\imath}(\lambda))^{\frac{2-\gamma_{1}}{2}}.
\end{aligned}
\tag{13}
$$

Similarly,

$$
\begin{aligned}
2c_{1}\sum_{\imath=1}^{M}\hat{\boldsymbol{e}}_{\imath}^{T}(\lambda)\boldsymbol{X}^{\frac{2+\gamma_{1}}{2}}\mathbf{sign}(\hat{\boldsymbol{e}}_{\imath}(\lambda))|\hat{\boldsymbol{e}}_{\imath}(\lambda)|^{1+\gamma_{1}}=&2c_{1}\sum_{\imath=1}^{M}\sum_{s=1}^{n}X_{s}^{\frac{2+\gamma_{1}}{2}}|\hat{e}_{\imath s}(\lambda)|^{2+\gamma_{1}}\\
\geq&2\frac{c_{1}}{n^{\frac{\gamma_{1}}{2}}}\sum_{\imath=1}^{M}\left(\sum_{s=1}^{n}X_{s}\hat{e}_{\imath s}^{2}(\lambda)\right)^{\frac{2+\gamma_{1}}{2}}\\
=&2\frac{c_{1}}{n^{\frac{\gamma_{1}}{2}}}\sum_{\imath=1}^{M}\left(\hat{\boldsymbol{e}}_{\imath}^{T}(\lambda)\boldsymbol{X}\hat{\boldsymbol{e}}_{\imath}(\lambda)\right)^{\frac{2+\gamma_{1}}{2}}.
\end{aligned}
\tag{14}
$$

$$
\begin{aligned}
2c_2\sum_{\imath=1}^{M}\hat{\boldsymbol{e}}_\imath^T(\lambda)\boldsymbol{X}^{\frac{2-\gamma_1}{2}}\mathbf{sign}(\hat{\boldsymbol{e}}_\imath(\lambda))|\hat{\boldsymbol{e}}_\imath(\lambda)|^{1-\gamma_1} =& 2c_2\sum_{\imath=1}^{M}\sum_{s=1}^{n}X_s^{\frac{2-\gamma_1}{2}}|\hat{e}_{\imath s}(\lambda)|^{2-\gamma_1}\\
\geq& 2c_2\sum_{\imath=1}^{M}\left(\sum_{s=1}^{n}X_s\hat{e}_{\imath s}^2(\lambda)\right)^{\frac{2-\gamma_1}{2}}\\
=& 2c_2\sum_{\imath=1}^{M}(\hat{\boldsymbol{e}}_\imath^T(\lambda)\boldsymbol{X}\hat{\boldsymbol{e}}_\imath(\lambda))^{\frac{2-\gamma_1}{2}}.
\end{aligned}
\tag{15}
$$

According to (9) - (15), one can get

$$
\begin{aligned}
\dot{P}(\lambda)\leq& 2\sum_{\imath=1}^{M}\sum_{i=1}^{M}\rho Q_{\imath i}\boldsymbol{e}_\imath^T(\lambda)\boldsymbol{X}\boldsymbol{W}\boldsymbol{e}_\imath(\lambda)+\sum_{\imath=1}^{M}\hat{\boldsymbol{e}}_\imath^T(\lambda)(-2\boldsymbol{X}\boldsymbol{A}+\boldsymbol{X}\boldsymbol{B}\boldsymbol{B}^T\boldsymbol{X}+\boldsymbol{X}\boldsymbol{G})\hat{\boldsymbol{e}}_\imath(\lambda)\\
&+2\sum_{\imath=1}^{M}\sum_{i=1}^{M}\varrho H_{\imath i}\hat{\boldsymbol{e}}_\imath^T(\lambda)\boldsymbol{X}\boldsymbol{\Gamma}\hat{\boldsymbol{e}}_\imath(\lambda)+\sum_{\imath=1}^{M}\boldsymbol{e}_\imath^T(\lambda)(-2\boldsymbol{X}\boldsymbol{C}+\boldsymbol{X}\boldsymbol{D}\boldsymbol{D}^T\boldsymbol{X}+2\boldsymbol{\Psi}+\boldsymbol{X}\boldsymbol{G})\boldsymbol{e}_\imath(\lambda)\\
&-2c_1\sum_{\imath=1}^{M}(\boldsymbol{e}_\imath^T(\lambda)\boldsymbol{X}\boldsymbol{e}_\imath(\lambda))^{\frac{2+\gamma_1}{2}}-2c_1\sum_{\imath=1}^{M}(\hat{\boldsymbol{e}}_\imath^T(\lambda)\boldsymbol{X}\hat{\boldsymbol{e}}_\imath(\lambda))^{\frac{2+\gamma_1}{2}}-2\sum_{\imath=1}^{M}\boldsymbol{e}_\imath^T(\lambda)\boldsymbol{X}\boldsymbol{V}_\imath\boldsymbol{e}_\imath(\lambda)\\
&-2c_2\sum_{\imath=1}^{M}(\boldsymbol{e}_\imath^T(\lambda)\boldsymbol{X}\boldsymbol{e}_\imath(\lambda))^{\frac{2-\gamma_1}{2}}-2c_2\sum_{\imath=1}^{M}(\hat{\boldsymbol{e}}_\imath^T(\lambda)\boldsymbol{X}\hat{\boldsymbol{e}}_\imath(\lambda))^{\frac{2-\gamma_1}{2}}-2\sum_{\imath=1}^{M}\boldsymbol{e}_\imath^T(\lambda)\boldsymbol{X}\boldsymbol{V}_\imath\hat{\boldsymbol{e}}_\imath(\lambda)\\
\leq& \boldsymbol{e}^T(\lambda)\big[\boldsymbol{I_M}\otimes(-2\boldsymbol{X}\boldsymbol{C}+\boldsymbol{X}\boldsymbol{D}\boldsymbol{D}^T\boldsymbol{X}+2\boldsymbol{\Psi}+\boldsymbol{X}\boldsymbol{G})-(\boldsymbol{I_M}\otimes\boldsymbol{X})\boldsymbol{V}-\boldsymbol{V}^T(\boldsymbol{I_M}\otimes\boldsymbol{X})\\
&+\rho\boldsymbol{Q}\otimes(\boldsymbol{X}\boldsymbol{W}+\boldsymbol{W}^T\boldsymbol{X})\big]\boldsymbol{e}(\lambda)+\hat{\boldsymbol{e}}^T(\lambda)\big[\boldsymbol{I_M}\otimes(-2\boldsymbol{X}\boldsymbol{A}+\boldsymbol{X}\boldsymbol{B}\boldsymbol{B}^T\boldsymbol{X}+\boldsymbol{X}\boldsymbol{G})\\
&-(\boldsymbol{I_M}\otimes\boldsymbol{X})\boldsymbol{V}-\boldsymbol{V}^T(\boldsymbol{I_M}\otimes\boldsymbol{X})+\varrho\boldsymbol{H}\otimes(\boldsymbol{X}\boldsymbol{\Gamma}+\boldsymbol{\Gamma}^T\boldsymbol{X})\big]\hat{\boldsymbol{e}}(\lambda)\\
&-2\frac{c_1}{n^{\frac{\gamma_1}{2}}}\sum_{\imath=1}^{M}(\boldsymbol{e}_\imath^T(\lambda)\boldsymbol{X}\boldsymbol{e}_\imath(\lambda))^{\frac{2+\gamma_1}{2}}-2c_2\sum_{\imath=1}^{M}(\boldsymbol{e}_\imath^T(\lambda)\boldsymbol{X}\boldsymbol{e}_\imath(\lambda))^{\frac{2-\gamma_1}{2}}\\
&-2\frac{c_1}{n^{\frac{\gamma_1}{2}}}\sum_{\imath=1}^{M}(\hat{\boldsymbol{e}}_\imath^T(\lambda)\boldsymbol{X}\hat{\boldsymbol{e}}_\imath(\lambda))^{\frac{2-\gamma_1}{2}}-2c_2\sum_{\imath=1}^{M}(\hat{\boldsymbol{e}}_\imath^T(\lambda)\boldsymbol{X}\hat{\boldsymbol{e}}_\imath(\lambda))^{\frac{2-\gamma_1}{2}}\\
\leq& -2\frac{c_1}{n^{\frac{\gamma_1}{2}}}\sum_{\imath=1}^{M}(\boldsymbol{e}_\imath^T(\lambda)\boldsymbol{X}\boldsymbol{e}_\imath(\lambda))^{\frac{2+\gamma_1}{2}}-2c_2\sum_{\imath=1}^{M}(\boldsymbol{e}_\imath^T(\lambda)\boldsymbol{X}\boldsymbol{e}_\imath(\lambda))^{\frac{2-\gamma_1}{2}}\\
&-2\frac{c_1}{n^{\frac{\gamma_1}{2}}}\sum_{\imath=1}^{M}(\hat{\boldsymbol{e}}_\imath^T(\lambda)\boldsymbol{X}\hat{\boldsymbol{e}}_\imath(\lambda))^{\frac{2+\gamma_1}{2}}-2c_2\sum_{\imath=1}^{M}(\hat{\boldsymbol{e}}_\imath^T(\lambda)\boldsymbol{X}\hat{\boldsymbol{e}}_\imath(\lambda))^{\frac{2-\gamma_1}{2}}\\
\leq& -2\frac{c_1}{(nM)^{\frac{\gamma_1}{2}}}\left(\sum_{\imath=1}^{M}\boldsymbol{e}_\imath^T(\lambda)\boldsymbol{X}\boldsymbol{e}_\imath(\lambda)\right)^{\frac{2+\gamma_1}{2}}-2\frac{c_1}{(nM)^{\frac{\gamma_1}{2}}}\left(\sum_{\imath=1}^{M}\hat{\boldsymbol{e}}_\imath^T(\lambda)\boldsymbol{X}\hat{\boldsymbol{e}}_\imath(\lambda)\right)^{\frac{2+\gamma_1}{2}}\\
&-2c_2\left(\sum_{\imath=1}^{M}\boldsymbol{e}_\imath^T(\lambda)\boldsymbol{X}\boldsymbol{e}_\imath(\lambda)\right)^{\frac{2-\gamma_1}{2}}-2c_2\left(\sum_{\imath=1}^{M}\hat{\boldsymbol{e}}_\imath^T(\lambda)\boldsymbol{X}\hat{\boldsymbol{e}}_\imath(\lambda)\right)^{\frac{2-\gamma_1}{2}}\\
=& -2\frac{c_1}{(nM)^{\frac{\gamma_1}{2}}}\left[P_1^{\frac{2+\gamma_1}{2}}(\lambda)+P_2^{\frac{2+\gamma_1}{2}}(\lambda)\right]-2c_2\left[P_1^{\frac{2-\gamma_1}{2}}(\lambda)+P_2^{\frac{2-\gamma_1}{2}}(\lambda)\right]\\
\leq& -\frac{2c_1}{(2nM)^{\frac{\gamma_1}{2}}}\left[P_1(\lambda)+P_2(\lambda)\right]^{\frac{2+\gamma_1}{2}}-2c_2\left[P_1(\lambda)+P_2(\lambda)\right]^{\frac{2-\gamma_1}{2}}.
\end{aligned}
$$

Since $c_1=\frac{\pi(nM)^{\frac{\gamma_1}{2}}}{2^{\frac{2-\gamma_1}{2}}\gamma_1T_c}$ and $c_2=\frac{\pi}{2\gamma_1T_c}$, one has

$$
\begin{aligned}
&-\frac{2c_1}{(2nM)^{\frac{\gamma_1}{2}}}\left[P_1(\lambda)+P_2(\lambda)\right]^{\frac{2+\gamma_1}{2}}-2c_2\left[P_1(\lambda)+P_2(\lambda)\right]^{\frac{2-\gamma_1}{2}}\\
=&-\frac{\pi}{\gamma_1T_c}\left(P^{1+\frac{\gamma_1}{2}}(\lambda)+P^{1-\frac{\gamma_1}{2}}(\lambda)\right).
\end{aligned}
\tag{16}
$$

It then follows from Lemma 1 that the drive and response systems (3) and (4) realize predefined-time synchronization with predefined-time T_c under the action of the bilayer controllers (6).

Remark 2. To achieve better performance in synchronization, extensive research has been conducted on finite-time and fixed-time synchronization as alternatives to conventional asymptotic and exponential synchronization [6, 7, 12, 15, 16, 18, 19, 20, 21, 22, 23]. However, the synchronization time in finite-time synchronization is the value of the settling time function which is easy to change with initial value. Moreover, it is difficult to obtain the exact initial value of the actual system. As a special case of finite-time synchronization, fixed-time synchronization has a definite upper bound on the settling time, which is independent of the initial value of the system. However, the convergence time in fixed-time synchronization is not convenient to regulate based on the parameters of system and controller. Fortunately, predefined-time synchronization can solve the above problem, and in which the settling time does not depend on any initial value and it can be configured as a controller parameter. As far as we know, only the traditional synchronization [17] and finite-time synchronization [18] for coupled competitive NNs have been investigated before, no research results have been reported on the predefined-time synchronization of this kind of network. In Theorem 1, a novel predefined-time synchronization criterion is established for drive and response systems of coupled competitive NNs by constructing a new bilayer controller.

4 | PREDEFINED-TIME SYNCHRONIZATION OF COUPLED COMPETITIVE NNS WITH TIME-VARYING DELAYS

This section is devoted to studying the coupled competitive NNs with time-varying delays, which is given by

$$\begin{cases} STM : \dot{\boldsymbol{y}}_\imath(\lambda) = -\boldsymbol{C}\boldsymbol{y}_\imath(\lambda) + \boldsymbol{D}\boldsymbol{f}(\overline{\boldsymbol{y}_\imath(\lambda)}) + \boldsymbol{G}\boldsymbol{\theta}_\imath(\lambda) + \rho\sum_{i=1}^{M} Q_{\imath i}\boldsymbol{W}\boldsymbol{y}_i(\lambda), \\ LTM : \dot{\boldsymbol{\theta}}_\imath(\lambda) = -\boldsymbol{A}\boldsymbol{\theta}_\imath(\lambda) + \boldsymbol{B}\boldsymbol{f}(\boldsymbol{y}_\imath(\lambda)) + \varrho\sum_{i=1}^{N} H_{\imath i}\boldsymbol{\Gamma}\boldsymbol{\theta}_i(\lambda), \end{cases} \tag{17}$$

where $\imath = 1, 2, \cdots, M$; $\overline{\boldsymbol{y}_\imath(\lambda)} = (y_{\imath 1}(\lambda-\tau_1(\lambda)), y_{\imath 2}(\lambda-\tau_2(\lambda)), \cdots, y_{\imath n}(\lambda-\tau_n(\lambda)))^T \in \mathbb{R}^n$, $\tau_s(\lambda)$ $(s = 1, 2, \cdots, n)$ is the time-varying delay with $0 \le \tau_s(\lambda) \le \tau_s \le \tau = \max_{s=1,2,\cdots,n}\{\tau_j\}$ and $\dot{\tau}_s(\lambda) \le \epsilon_s < 1$; $\boldsymbol{f}(\overline{\boldsymbol{y}_\imath(\lambda)}) = (f_1(y_{\imath 1}(\lambda-\tau_1(\lambda))), f_2(y_{\imath 2}(\lambda-\tau_2(\lambda))), \cdots, f_n(y_{\imath n}(\lambda-\tau_n(\lambda))))^T$; $f_s(y_{\imath s}(\lambda-\tau_s(\lambda)))$ is the activation function of the s-th neuron at the time $t-\tau_s(t)$; $\boldsymbol{y}_\imath(\lambda), \boldsymbol{C}, \boldsymbol{D}, \boldsymbol{G}, \boldsymbol{\theta}_\imath(\lambda), \rho, Q_{\imath i}$, $\boldsymbol{W}, \boldsymbol{A}, \boldsymbol{B}, \varrho, H_{\imath i}, \boldsymbol{\Gamma}$ have the same meanings as in Section 3. For convenience, denote $\boldsymbol{\Xi} = \mathrm{diag}(\frac{1}{1-\epsilon_1}, \frac{1}{1-\epsilon_2}, \cdots, \frac{1}{1-\epsilon_n})$.

In this section, let system (17) be a drive system, its corresponding response system can be represented by

$$\begin{cases} STM : \dot{\boldsymbol{z}}_\imath(\lambda) = -\boldsymbol{C}\boldsymbol{z}_\imath(\lambda) + \boldsymbol{D}\boldsymbol{f}(\overline{\boldsymbol{z}_\imath(\lambda)}) + \rho\sum_{i=1}^{M} Q_{\imath i}\boldsymbol{W}\boldsymbol{z}_i(\lambda) + \boldsymbol{G}\boldsymbol{\delta}_\imath(\lambda) + \boldsymbol{u}_\imath(\lambda), \\ LTM : \dot{\boldsymbol{\delta}}_\imath(\lambda) = -\boldsymbol{A}\boldsymbol{\delta}_\imath(\lambda) + \boldsymbol{B}\boldsymbol{f}(\boldsymbol{z}_\imath(\lambda)) + \varrho\sum_{i=1}^{M} H_{\imath i}\boldsymbol{\Gamma}\boldsymbol{\delta}_i(\lambda) + \boldsymbol{m}_\imath(\lambda), \end{cases} \tag{18}$$

where $\imath = 1, 2, \cdots, M$; $\overline{\boldsymbol{z}_\imath(\lambda)} = (z_{\imath 1}(\lambda-\tau_1(\lambda)), z_{\imath 2}(\lambda-\tau_2(\lambda)), \cdots, z_{\imath n}(\lambda-\tau_n(\lambda)))^T \in \mathbb{R}^n$; $\boldsymbol{f}(\overline{\boldsymbol{z}_\imath(\lambda)}) = (f_1(z_{\imath 1}(\lambda-\tau_1(\lambda))), f_2(z_{\imath 2}(\lambda-\tau_2(\lambda))), \cdots, f_n(z_{\imath n}(\lambda-\tau_n(\lambda))))^T$; $f_j(z_{\imath s}(\lambda-\tau_s(\lambda)))$ is the activation function of the s-th neuron at the time $t-\tau_s(\lambda)$; $\boldsymbol{u}_\imath(\lambda)$ and $\boldsymbol{m}_\imath(\lambda)$ are the controllers to be designed; $\boldsymbol{z}_\imath(\lambda), \boldsymbol{C}, \boldsymbol{A}, \boldsymbol{B}, \boldsymbol{D}, \boldsymbol{G}, \boldsymbol{\delta}_\imath(t), \rho, \varrho, Q_{\imath i}, H_{\imath i}, \boldsymbol{\Gamma}, \boldsymbol{W}$ have the same meanings as in network (4).

Let $\boldsymbol{e}_\imath(\lambda) = \boldsymbol{z}_\imath(\lambda) - \boldsymbol{y}_\imath(\lambda)$ and $\hat{\boldsymbol{e}}_\imath(\lambda) = \boldsymbol{\delta}_\imath(\lambda) - \boldsymbol{\theta}_\imath(\lambda)$, then the description of the error system can be expressed by the following equations:

$$\begin{cases} \dot{\boldsymbol{e}}_\imath(\lambda) = -\boldsymbol{C}\boldsymbol{e}_\imath(\lambda) + \boldsymbol{D}[\boldsymbol{f}(\overline{\boldsymbol{z}_\imath(\lambda)}) - \boldsymbol{f}(\overline{\boldsymbol{y}_\imath(\lambda)})] + \boldsymbol{G}\hat{\boldsymbol{e}}_\imath(\lambda) + \rho\sum_{i=1}^{M} Q_{\imath i}\boldsymbol{W}\boldsymbol{e}_i(\lambda) + \boldsymbol{u}_\imath(\lambda), \\ \dot{\hat{\boldsymbol{e}}}_\imath(\lambda) = -\boldsymbol{A}\hat{\boldsymbol{e}}_\imath(\lambda) + \boldsymbol{B}[\boldsymbol{f}(\boldsymbol{z}_\imath(\lambda)) - \boldsymbol{f}(\boldsymbol{y}_\imath(\lambda))] + \boldsymbol{m}_\imath(\lambda) + \varrho\sum_{i=1}^{M} H_{\imath i}\boldsymbol{\Gamma}\hat{\boldsymbol{e}}_i(\lambda). \end{cases} \tag{19}$$

Design the following bilayer controllers for the network (19):

$$\begin{cases} \boldsymbol{u}_\iota(\lambda) = -c_1 \boldsymbol{X}^{\frac{\gamma_1}{2}} \mathbf{sign}(\boldsymbol{e}_\iota(\lambda))|\boldsymbol{e}_\iota(\lambda)|^{1+\gamma_1} - c_1 \boldsymbol{X}^{-1} \sum_{s=1}^{n} \left(\frac{\varpi_s^2}{1-\epsilon_s} \int_{\lambda-\tau_s(\lambda)}^{t} e_{\iota s}^2(h)dh \right)^{\frac{2+\gamma_1}{2}} \frac{\boldsymbol{e}_\iota(\lambda)}{\|\boldsymbol{e}_\iota(\lambda)\|^2} \\ \qquad - c_2 \boldsymbol{X}^{-1} \sum_{s=1}^{n} \left(\frac{\varpi_s^2}{1-\epsilon_s} \int_{\lambda-\tau_s(\lambda)}^{t} e_{\iota s}^2(h)dh \right)^{\frac{2-\gamma_1}{2}} \frac{\boldsymbol{e}_\iota(\lambda)}{\|\boldsymbol{e}_\iota(\lambda)\|^2} - c_2 \boldsymbol{X}^{-\frac{\gamma_1}{2}} \mathbf{sign}(\boldsymbol{e}_\iota(\lambda))|\boldsymbol{e}_\iota(\lambda)|^{1-\gamma_1} - \boldsymbol{V}_\iota \boldsymbol{e}_\iota(\lambda), \\ \boldsymbol{m}_\iota(\lambda) = -\frac{c_1}{2^{\frac{\gamma_1}{2}}} \boldsymbol{X}^{\frac{\gamma_1}{2}} \mathbf{sign}(\hat{\boldsymbol{e}}_\iota(\lambda))|\hat{\boldsymbol{e}}_\iota(\lambda)|^{1+\gamma_1} - \boldsymbol{V}_\iota \hat{\boldsymbol{e}}_\iota(\lambda) - c_2 \boldsymbol{X}^{-\frac{\gamma_1}{2}} \mathbf{sign}(\hat{\boldsymbol{e}}_\iota(\lambda))|\hat{\boldsymbol{e}}_\iota(\lambda)|^{1-\gamma_1}, \end{cases} \tag{20}$$

where $c_1 = \frac{\pi (nM)^{\frac{\gamma_1}{2}}}{2^{1-\gamma_1}\gamma_1 T_c}$, c_2, $\boldsymbol{X}$, $\boldsymbol{X}^{\frac{\gamma_1}{2}}$, $\boldsymbol{X}^{-\frac{\gamma_1}{2}}$, γ_1, $\mathbf{sign}(\boldsymbol{e}_s(\lambda))$, $|\boldsymbol{e}_s\lambda)|^{1+\gamma_1}$, $|\boldsymbol{e}_s(\lambda)|^{1-\gamma_1}$, $\boldsymbol{V}_\iota$ have the identical meanings as in (6).

Remark 3. In this paper, two novel bilayer controllers (6) and (20) are well designed for achieving predefined-time synchronization of the drive-response error systems (5) and (19) respectively. Actually, these controllers are designed by improving some existing controllers in [7, 12, 16, 23, 26] for finite/fixed/predefined-time synchronization and utilizing the own characteristics of our network models. The innovation of our proposed controllers (6) is mainly reflected in the following two aspects: (i) the coefficient or parameter before each item in the controller is different from some existing controllers; (ii) our controller is two-layer. More precisely, in view of the bilayer structure of coupled competitive NNs, bilayer predefined-time controller should be designed for STM and LTM respectively. Actually, they are designed by leveraging the unique structural characteristics of coupled competitive NNs, allowing for more effective management of interactions between STM and LTM, which is crucial for achieving synchronization. Compared to single-layer controller, bilayer controller can enhance control efficacy, ultimately leading to more effective synchronization outcomes. Furthermore, for achieving predefined-time synchronization of the considered networks, the controller's parameters must be designed as functions of the predefined time so that it can be configured in advance according to different requirements. For coupled competitive NNs with time-varying delays, the controllers (20) is designed by adding two new terms which relate to the bound of the derivative of time-varying delay based on controllers (6). Note that the term $\frac{e_\iota(\lambda)}{\|e_\iota(\lambda)\|^2}$ is contained in these new added terms in controller $\boldsymbol{u}_\iota(\lambda)$ of (20). As all nodes must synchronize to the target during the synchronization process, i.e., $\boldsymbol{e}_\iota(\lambda) \to 0$, the magnitude of $\frac{e_\iota(\lambda)}{\|e_\iota(\lambda)\|^2}$ will approach infinity, which lead to singularity and abruptness easily. To avoid the occurrence of these undesirable phenomena in practice, a sufficient small positive constant χ can be added to the denominator as in some existing works, i.e., $\frac{e_\iota(\lambda)}{\|e_\iota(\lambda)\|^2}$ is replacing by $\frac{e_\iota(\lambda)}{\|e_\iota(\lambda)\|^2+\chi}$. Additionally, the term $\mathrm{sign}(e_{\iota s}(\lambda))$ in diagonal matrix $\mathbf{sign}(\boldsymbol{e}_\iota(\lambda))$ of the designed controllers (6) and (20) is discontinuous, which will lead to some undesirable chattering phenomenon in reality. In practical applications, these discontinuous term $\mathrm{sign}(e_{\iota s}(\lambda))$ is usually approximated by $\frac{e_{\iota s}(\lambda)}{e_{\iota s}(\lambda)+\zeta}$, where $\zeta > 0$ is a sufficiently small constant.

Theorem 2. Under the bilayer controllers (20), the network (19) achieves predefined-time synchronization if there are two matrices $0 < \boldsymbol{X} = \mathrm{diag}(X_1, X_2, \cdots, X_n) \in \mathbb{R}^{n\times n}$, $\boldsymbol{V} = \mathrm{diag}(V_1, V_2, \cdots, V_M) \in \mathbb{R}^{nM\times nM}$ such that

$$\begin{cases} \boldsymbol{I_M} \otimes \hat{\boldsymbol{\Upsilon}}_1 - (\boldsymbol{I_M} \otimes \boldsymbol{X})\boldsymbol{V} - \boldsymbol{V}^T(\boldsymbol{I_M} \otimes \boldsymbol{X}) + \rho \boldsymbol{Q} \otimes (\boldsymbol{XW} + \boldsymbol{W}^T\boldsymbol{X}) < 0, \\ \boldsymbol{I_M} \otimes \hat{\boldsymbol{\Upsilon}}_2 - (\boldsymbol{I_M} \otimes \boldsymbol{X})\boldsymbol{V} - \boldsymbol{V}^T(\boldsymbol{I_M} \otimes \boldsymbol{X}) + \varrho \boldsymbol{H} \otimes (\boldsymbol{X\Gamma} + \boldsymbol{\Gamma}^T\boldsymbol{X}) < 0, \end{cases} \tag{21}$$

where $\hat{\boldsymbol{\Upsilon}}_1 = -2\boldsymbol{XC} + \boldsymbol{XDD}^T\boldsymbol{X} + \boldsymbol{\Psi\Xi} + \boldsymbol{\Psi} + \boldsymbol{XG}$, $\hat{\boldsymbol{\Upsilon}}_2 = -2\boldsymbol{XA} + \boldsymbol{XBB}^T\boldsymbol{X} + \boldsymbol{XG}$.

Proof. For error system (19), the Lyapunov functional is constructed as follows:

$$\hat{P}(\lambda) = \hat{P}_1(\lambda) + \hat{P}_2(\lambda), \tag{22}$$

where

$$\hat{P}_1(\lambda) = \sum_{\iota=1}^{M} \boldsymbol{e}_\iota^T(\lambda)\boldsymbol{X}\boldsymbol{e}_\iota(\lambda) + \sum_{\iota=1}^{M}\sum_{s=1}^{n} \frac{\varpi_s^2}{1-\epsilon_s} \int_{\lambda-\tau_s(\lambda)}^{t} e_{\iota s}^2(h)dh,$$

$$\hat{P}_2(\lambda) = \sum_{\iota=1}^{M} \hat{\boldsymbol{e}}_\iota^T(\lambda)\boldsymbol{X}\hat{\boldsymbol{e}}_\iota(\lambda).$$

Consequently, one obtains

$$\begin{aligned}\dot{\hat{P}}(\lambda) =&2\sum_{\imath=1}^{M} \boldsymbol{e}_\imath^T(\lambda)\boldsymbol{X}\dot{\boldsymbol{e}}_\imath(\lambda) + \sum_{\imath=1}^{M}\sum_{s=1}^{n}\frac{\varpi_s^2}{1-\epsilon_s}e_{\imath s}^2(\lambda) + 2\sum_{\imath=1}^{M}\hat{\boldsymbol{e}}_\imath^T(\lambda)\boldsymbol{X}\dot{\hat{\boldsymbol{e}}}_\imath(\lambda)\\
&-\sum_{\imath=1}^{M}\sum_{s=1}^{n}\frac{\varpi_s^2}{1-\epsilon_s}e_{\imath s}^2(\lambda-\tau_s(\lambda))(1-\dot{\tau}_s(\lambda))\\
\leq&2\sum_{\imath=1}^{M}\boldsymbol{e}_\imath^T(\lambda)\boldsymbol{X}\big[-\boldsymbol{C}\boldsymbol{e}_\imath(\lambda)+\boldsymbol{D}(\boldsymbol{f}(\overline{\boldsymbol{z}_\imath(\lambda)})-\boldsymbol{f}(\overline{\boldsymbol{y}_\imath(\lambda)}))+\boldsymbol{G}\hat{\boldsymbol{e}}_\imath(\lambda)\\
&-c_1\boldsymbol{X}^{\frac{\gamma_1}{2}}\mathbf{sign}(\boldsymbol{e}_\imath(\lambda))|\boldsymbol{e}_\imath(\lambda)|^{1+\gamma_1}-c_2\boldsymbol{X}^{-\frac{\gamma_1}{2}}\mathbf{sign}(\boldsymbol{e}_\imath(\lambda))|\boldsymbol{e}_\imath(\lambda)|^{1-\gamma_1}\\
&-c_1\boldsymbol{X}^{-1}\sum_{s=1}^{n}\left(\frac{\varpi_s^2}{1-\epsilon_s}\int_{\lambda-\tau_s(\lambda)}^{t}e_{\imath s}^2(h)dh\right)^{\frac{2+\gamma_1}{2}}\frac{\boldsymbol{e}_\imath(\lambda)}{\|\boldsymbol{e}_\imath(\lambda)\|^2}\\
&-c_2\boldsymbol{X}^{-1}\sum_{s=1}^{n}\left(\frac{\varpi_s^2}{1-\epsilon_s}\int_{\lambda-\tau_s(\lambda)}^{t}e_{\imath s}^2(h)dh\right)^{\frac{2-\gamma_1}{2}}\frac{\boldsymbol{e}_\imath(\lambda)}{\|\boldsymbol{e}_\imath(\lambda)\|^2}\\
&-\boldsymbol{V}_\imath\boldsymbol{e}_\imath(\lambda)+\rho\sum_{i=1}^{M}Q_{\imath i}\boldsymbol{W}\boldsymbol{e}_i(\lambda)\big]+\sum_{\imath=1}^{M}\boldsymbol{e}_\imath^T(\lambda)\boldsymbol{\Psi}\boldsymbol{\Xi}\boldsymbol{e}_\imath(\lambda)\\
&-\sum_{\imath=1}^{M}\overline{\boldsymbol{e}_\imath^T(\lambda)}\boldsymbol{\Psi}\overline{\boldsymbol{e}_\imath(\lambda)}+2\sum_{\imath=1}^{M}\hat{\boldsymbol{e}}_\imath^T(\lambda)\boldsymbol{X}\big[-\boldsymbol{A}\hat{\boldsymbol{e}}_\imath(\lambda)-\boldsymbol{V}_\imath\hat{\boldsymbol{e}}_\imath(\lambda)\\
&+\boldsymbol{B}(\boldsymbol{f}(\boldsymbol{z}_\imath(\lambda))-\boldsymbol{f}(\boldsymbol{y}_\imath(\lambda)))-\frac{c_1}{2^{\frac{\gamma_1}{2}}}\boldsymbol{X}^{\frac{\gamma_1}{2}}\mathbf{sign}(\hat{\boldsymbol{e}}_\imath(\lambda))|\hat{\boldsymbol{e}}_\imath(\lambda)|^{1+\gamma_1}\\
&-c_2\boldsymbol{X}^{-\frac{\gamma_1}{2}}\mathbf{sign}(\hat{\boldsymbol{e}}_\imath(\lambda))|\hat{\boldsymbol{e}}_\imath(\lambda)|^{1-\gamma_1}+\varrho\sum_{i=1}^{M}H_{\imath i}\boldsymbol{\Gamma}\hat{\boldsymbol{e}}_i(\lambda)\big].\end{aligned} \tag{23}$$

Based on Assumption 1 and Lemma 3, one gets

$$\begin{aligned}2\boldsymbol{e}_\imath^T(\lambda)\boldsymbol{X}\boldsymbol{D}(\boldsymbol{f}(\overline{\boldsymbol{z}_\imath(\lambda)})-\boldsymbol{f}(\overline{\boldsymbol{y}_\imath(\lambda)}))\leq&\,\boldsymbol{e}_\imath^T(\lambda)\boldsymbol{X}\boldsymbol{D}\boldsymbol{D}^T\boldsymbol{X}\boldsymbol{e}_\imath(\lambda)+(\boldsymbol{f}(\overline{\boldsymbol{z}_\imath(\lambda)})-\boldsymbol{f}(\overline{\boldsymbol{y}_\imath(\lambda)}))^T(\boldsymbol{f}(\overline{\boldsymbol{z}_\imath(\lambda)})-\boldsymbol{f}(\overline{\boldsymbol{y}_\imath(\lambda)}))\\
=&\,\boldsymbol{e}_\imath^T(\lambda)\boldsymbol{X}\boldsymbol{D}\boldsymbol{D}^T\boldsymbol{X}\boldsymbol{e}_\imath(\lambda)+\sum_{s=1}^{n}(f_s(\overline{z_{\imath s}(\lambda)})-f_s(\overline{y_{\imath s}(\lambda)}))^2\\
\leq&\,\boldsymbol{e}_\imath^T(\lambda)\boldsymbol{X}\boldsymbol{D}\boldsymbol{D}^T\boldsymbol{X}\boldsymbol{e}_\imath(\lambda)+\sum_{s=1}^{n}\varpi_s^2(\overline{z_{\imath s}(\lambda)}-\overline{y_{\imath s}(\lambda)})^2\\
=&\,\boldsymbol{e}_\imath^T(\lambda)\boldsymbol{X}\boldsymbol{D}\boldsymbol{D}^T\boldsymbol{X}\boldsymbol{e}_\imath(\lambda)+\sum_{s=1}^{n}\varpi_s^2\overline{e_{\imath s}(\lambda)}^2\\
=&\,\boldsymbol{e}_\imath^T(\lambda)\boldsymbol{X}\boldsymbol{D}\boldsymbol{D}^T\boldsymbol{X}\boldsymbol{e}_\imath(\lambda)+\overline{\boldsymbol{e}_\imath^T(\lambda)}\boldsymbol{\Psi}\overline{\boldsymbol{e}_\imath(\lambda)}.\end{aligned} \tag{24}$$

Moreover,

$$\begin{aligned}&2\frac{c_1}{2^{\frac{\gamma_1}{2}}}\sum_{\imath=1}^{M}\hat{\boldsymbol{e}}_\imath^T(\lambda)\boldsymbol{X}^{\frac{2+\gamma_1}{2}}\mathbf{sign}(\hat{\boldsymbol{e}}_\imath(\lambda))|\hat{\boldsymbol{e}}_\imath(\lambda)|^{1+\gamma_1}\\
&=2\frac{c_1}{2^{\frac{\gamma_1}{2}}}\sum_{\imath=1}^{M}\sum_{s=1}^{n}X_s^{\frac{2+\gamma_1}{2}}|\hat{e}_{\imath s}(\lambda)|^{2+\gamma_1}\\
&\geq 2\frac{c_1}{(2n)^{\frac{\gamma_1}{2}}}\sum_{\imath=1}^{M}\left(\sum_{s=1}^{n}X_s\hat{e}_{\imath s}^2(\lambda)\right)^{\frac{2+\gamma_1}{2}}\\
&=2\frac{c_1}{(2n)^{\frac{\gamma_1}{2}}}\sum_{\imath=1}^{M}\left(\hat{\boldsymbol{e}}_\imath^T(\lambda)\boldsymbol{X}\hat{\boldsymbol{e}}_\imath(\lambda)\right)^{\frac{2+\gamma_1}{2}}.\end{aligned} \tag{25}$$

From (10)-(15) and (24)-(25), one can acquire

$$
\begin{aligned}
\dot{P}_2(\lambda) \le& \sum_{\iota=1}^{M} e_\iota^T(\lambda)(-2XC + XDD^TX + \Psi + \Psi\Xi + XG)e_\iota(\lambda) - 2\sum_{\iota=1}^{M} e_\iota^T(\lambda)XV_\iota e_\iota(\lambda) \\
&+ \sum_{\iota=1}^{M} \hat{e}_\iota^T(\lambda)(-2XA + XBB^TX + XG)\hat{e}_\iota(\lambda) - 2\frac{c_1}{n^{\frac{\gamma_1}{2}}}\sum_{\iota=1}^{M}(e_\iota^T(\lambda)Xe_\iota(\lambda))^{\frac{2+\gamma_1}{2}} \\
&- 2c_2\sum_{\iota=1}^{M}(e_\iota^T(\lambda)Xe_\iota(\lambda))^{\frac{2-\gamma_1}{2}} + 2\sum_{\iota=1}^{M}\sum_{i=1}^{M}\rho Q_{\iota i}e_\iota^T(\lambda)XWe_i(\lambda) - 2\sum_{\iota=1}^{M}\hat{e}_\iota^T(\lambda)XV_\iota\hat{e}_\iota(\lambda) \\
&- 2\frac{c_1}{n^{\frac{\gamma_1}{2}}}\sum_{\iota=1}^{M}\left(\sum_{s=1}^{n}\frac{\varpi_s^2}{1-\epsilon_s}\int_{\lambda-\tau_s(\lambda)}^{\lambda} e_{\iota s}^2(h)dh\right)^{\frac{2+\gamma_1}{2}} - 2\frac{c_1}{(2n)^{\frac{\gamma_1}{2}}}\sum_{\iota=1}^{M}(\hat{e}_\iota^T(\lambda)X\hat{e}_\iota(\lambda))^{\frac{2+\gamma_1}{2}} \\
&- 2c_2\sum_{\iota=1}^{M}(\hat{e}_\iota^T(\lambda)X\hat{e}_\iota(\lambda))^{\frac{2-\gamma_1}{2}} + 2\sum_{\iota=1}^{M}\sum_{i=1}^{M}\varrho H_{\iota i}\hat{e}_\iota^T(\lambda)X\Gamma\hat{e}_i(\lambda) \\
&- 2c_2\sum_{\iota=1}^{M}\left(\sum_{s=1}^{n}\frac{\varpi_s^2}{1-\epsilon_s}\int_{\lambda-\tau_s(\lambda)}^{\lambda} e_{\iota s}^2(h)dh\right)^{\frac{2-\gamma_1}{2}} \\
\le& e^T(\lambda)[I_M \otimes (-2XC + XDD^TX + \Psi\Xi + \Psi + XG) - (I_M \otimes X)V - V^T(I_M \otimes X) \\
&+ \rho Q \otimes (XW + W^TX)]e(\lambda) + \hat{e}^T(\lambda)[I_M \otimes (-2XA + XBB^TX + XG) \\
&- (I_M \otimes X)V - V^T(I_M \otimes X) + \varrho H \otimes (X\Gamma + \Gamma^TX)]\hat{e}(\lambda) \\
&- 2\frac{c_1}{n^{\frac{\gamma_1}{2}}}\left[\sum_{\iota=1}^{M}\left(\sum_{s=1}^{n}\frac{\varpi_s^2}{1-\epsilon_s}\int_{\lambda-\tau_s(\lambda)}^{\lambda} e_{\iota s}^2(h)dh\right)^{\frac{2+\gamma_1}{2}} + \sum_{\iota=1}^{M}(e_\iota^T(\lambda)Xe_\iota(\lambda))^{\frac{2+\gamma_1}{2}}\right] \\
&- 2c_2\left[\sum_{\iota=1}^{M}(e_\iota^T(\lambda)Xe_\iota(\lambda))^{\frac{2-\gamma_1}{2}} + \sum_{\iota=1}^{M}\left(\sum_{s=1}^{n}\frac{\varpi_s^2}{1-\epsilon_s}\int_{\lambda-\tau_s(\lambda)}^{t} e_{\iota s}^2(h)dh\right)^{\frac{2-\gamma_1}{2}}\right] \\
&- 2\frac{c_1}{(2n)^{\frac{\gamma_1}{2}}}\sum_{\iota=1}^{M}(\hat{e}_\iota^T(\lambda)X\hat{e}_\iota(\lambda))^{\frac{2+\gamma_1}{2}} - 2c_2\sum_{\iota=1}^{M}(\hat{e}_\iota^T(\lambda)X\hat{e}_\iota(\lambda))^{\frac{2-\gamma_1}{2}} \\
\le& -\frac{2^{\frac{2-\gamma_1}{2}}c_1}{(nM)^{\frac{\gamma_1}{2}}}\left(\sum_{\iota=1}^{M}\hat{e}_\iota^T(\lambda)X\hat{e}_\iota(\lambda)\right)^{\frac{2+\gamma_1}{2}} - 2c_2\left(\sum_{\iota=1}^{M}\hat{e}_\iota^T(\lambda)X\hat{e}_\iota(\lambda)\right)^{\frac{2-\gamma_1}{2}} \\
&- \frac{2c_1}{(nM)^{\frac{\gamma_1}{2}}}\left[\left(\sum_{\iota=1}^{M}\sum_{s=1}^{n}\frac{\varpi_s^2}{1-\epsilon_s}\int_{\lambda-\tau_s(\lambda)}^{\lambda} e_{\iota s}^2(h)dh\right)^{\frac{2+\gamma_1}{2}} + \left(\sum_{\iota=1}^{M}e_\iota^T(\lambda)Xe_\iota(\lambda)\right)^{\frac{2+\gamma_1}{2}}\right] \\
&- 2c_2\left[\left(\sum_{\iota=1}^{M}e_\iota^T(\lambda)Xe_\iota(\lambda)\right)^{\frac{2-\gamma_1}{2}} + \left(\sum_{\iota=1}^{M}\sum_{s=1}^{n}\frac{\varpi_s^2}{1-\epsilon_s}\int_{\lambda-\tau_s(\lambda)}^{\lambda} e_{\iota s}^2(h)dh\right)^{\frac{2-\gamma_1}{2}}\right] \\
\le& -\frac{2^{\frac{2-\gamma_1}{2}}c_1}{(nM)^{\frac{\gamma_1}{2}}}\left(\sum_{\iota=1}^{M}\hat{e}_\iota^T(\lambda)X\hat{e}_\iota(\lambda)\right)^{\frac{2+\gamma_1}{2}} - 2c_2\left(\sum_{\iota=1}^{M}\hat{e}_\iota^T(\lambda)X\hat{e}_\iota(\lambda)\right)^{\frac{2-\gamma_1}{2}} \\
&- \frac{2^{\frac{2-\gamma_1}{2}}c_1}{(nM)^{\frac{\gamma_1}{2}}}\left(\sum_{\iota=1}^{M}\sum_{s=1}^{n}\frac{\varpi_s^2}{1-\epsilon_s}\int_{\lambda-\tau_s(\lambda)}^{\lambda} e_{\iota s}^2(h)dh + \sum_{\iota=1}^{M}e_\iota^T(\lambda)Xe_\iota(\lambda)\right)^{\frac{2+\gamma_1}{2}}
\end{aligned}
$$

$$
\begin{aligned}
& -2c_2\left(\sum_{\iota=1}^{M} \boldsymbol{e}_\iota^T(\lambda)\boldsymbol{X}\boldsymbol{e}_\iota(\lambda)+\sum_{\iota=1}^{M}\sum_{s=1}^{n}\frac{\varpi_s^2}{1-\epsilon_s}\int_{\lambda-\tau_s(\lambda)}^{t} e_{\iota s}^2(h)dh\right)^{\frac{2-\gamma_1}{2}} \\
=& -\frac{2^{\frac{2-\gamma_1}{2}}c_1}{(nM)^{\frac{\gamma_1}{2}}}\left[\hat{P}_1^{\frac{2+\gamma_1}{2}}(\lambda)+\hat{P}_2^{\frac{2+\gamma_1}{2}}(\lambda)\right]-2c_2\left[\hat{P}_1^{\frac{2-\gamma_1}{2}}(\lambda)+\hat{P}_2^{\frac{2-\gamma_1}{2}}(\lambda)\right] \\
\leq& -\frac{2^{1-\gamma_1}c_1}{(nM)^{\frac{\gamma_1}{2}}}\left[\hat{P}_1(\lambda)+\hat{P}_2(\lambda)\right]^{\frac{2+\gamma_1}{2}}-2c_2\left[\hat{P}_1(\lambda)+\hat{P}_2(\lambda)\right]^{\frac{2-\gamma_1}{2}}.
\end{aligned}
$$

According to $c_1=\frac{\pi(nM)^{\frac{\gamma_1}{2}}}{\gamma_1 T_c 2^{1-\gamma_1}}$, $c_2=\frac{\pi}{2\gamma_1 T_c}$, one has

$$
\begin{aligned}
& -\frac{2^{1-\gamma_1}c_1}{(nM)^{\frac{\gamma_1}{2}}}\left[\hat{P}_1(\lambda)+\hat{P}_2(\lambda)\right]^{\frac{2+\gamma_1}{2}}-2c_2\left[\hat{P}_1(\lambda)+\hat{P}_2(\lambda)\right]^{\frac{2-\gamma_1}{2}} \\
=& -\frac{\pi}{\gamma_1 T_c}\left(\hat{P}^{1+\frac{\gamma_1}{2}}(\lambda)+\hat{P}^{1-\frac{\gamma_1}{2}}(\lambda)\right).
\end{aligned}
$$

Based on Lemma 1, the drive-response systems (17) and (18) reach predefined-time synchronization under the control of (20).

Remark 4. It follows from Theorems 1 and 2 that the coupled competitive NNs without and with time-varying delays achieve synchronization in the predefined time T_c independently of the initial values. Moreover, the predefined time T_c can be adjusted as a specific parameter in the designed bilayer predefined-time controllers. Thus, it can be an arbitrary positive constant. Based on real-world requirements, the predefined time T_c (the upper bound of the synchronization time) can be tuned arbitrarily. Therefore, predefined-time synchronization is superior to the other traditional synchronization methods, such as asymptotic synchronization and finite/fixed-time synchronization.

Remark 5. In the course of this study, the design of appropriate controllers and the construction of suitable Lyapunov functionals for the corresponding coupled competitive NNs are of primary importance for establishing predefined-time synchronization conditions. These novel bilayer controllers designed in this paper involved extensive testing of parameter settings to achieve synchronization in the desired convergence time. The necessity and advantages of designing bilayer controllers in this paper have been discussed in Remark 3. Additionally, how to find an appropriate Lyapunov functional that satisfies the necessary conditions for proving synchronization is also very challenging in this work. This paper constructs two Lyapunov functionals $P(\lambda)$ and $\hat{P}(\lambda)$ for achieving predefined-time synchronization of coupled competitive NNs without and with time-varying delays respectively, where $P(\lambda)$ is a single summation Lyapunov functional and $\hat{P}(\lambda)$ can be viewed as a double summation Lyapunov functional because the first term of $\hat{P}(\lambda)$ is a single summation. Although a single summation in Lyapunov functional $P(\lambda)$ may not capture all the intricacies of the system dynamics as effectively as higher-order summation terms, the proof based on it is more intuitive and easier to understand in the process of theoretical analysis. Due to the introduction of time-varying delays, a double summation Lyapunov functional $\hat{P}(\lambda)$ is designed to account for more elaborate time-delay and interaction effects. In the context of this study, the constructed Lyapunov functionals could simplify the mathematical analysis and reduce the computational complexity associated with deriving the predefined-time synchronization conditions, which have adequately addressed the stability and performance criteria required for the drive-response systems under consideration.

5 | NUMERICAL EXAMPLE

Example 5.1. Take the following drive and response systems of coupled competitive NNs into account:

$$
\begin{cases}
STM: \dot{\boldsymbol{y}}_\iota(\lambda)=-\boldsymbol{C}\boldsymbol{y}_\iota(\lambda)+\boldsymbol{D}\boldsymbol{f}(\boldsymbol{y}_\iota(\lambda))+\boldsymbol{G}\boldsymbol{\theta}_\iota(\lambda)+0.5\sum_{i=1}^{6}Q_{\iota i}\boldsymbol{W}\boldsymbol{y}_i(\lambda), \\
LTM: \dot{\boldsymbol{\theta}}_\iota(\lambda)=-\boldsymbol{A}\boldsymbol{\theta}_\iota(\lambda)+\boldsymbol{B}\boldsymbol{f}(\boldsymbol{y}_\iota(\lambda))+0.8\sum_{i=1}^{6}H_{\iota i}\boldsymbol{\Gamma}\boldsymbol{\theta}_i(\lambda),
\end{cases}
\tag{26}
$$

and

$$\begin{cases} STM: \dot{\boldsymbol{z}}_\iota(\lambda) = -\boldsymbol{C}\boldsymbol{z}_\iota(\lambda) + \boldsymbol{D}\boldsymbol{f}(\boldsymbol{z}_\iota(\lambda)) + 0.5\sum_{i=1}^{6} Q_{\iota i}\boldsymbol{W}\boldsymbol{z}_i(\lambda) + \boldsymbol{G}\boldsymbol{\delta}_\iota(\lambda) + \boldsymbol{u}_\iota(\lambda), \\ LTM: \dot{\boldsymbol{\delta}}_\iota(\lambda) = -\boldsymbol{A}\boldsymbol{\delta}_\iota(\lambda) + \boldsymbol{B}\boldsymbol{f}(\boldsymbol{z}_\iota(\lambda)) + 0.8\sum_{i=1}^{6} H_{\iota i}\boldsymbol{\Gamma}\boldsymbol{\delta}_i(\lambda) + \boldsymbol{m}_\iota(\lambda), \end{cases} \tag{27}$$

where $\iota = 1, 2, \cdots, 6$, $f_o(\phi) = \frac{|\phi+1|+|\phi-1|}{5} (o = 1, 2, 3)$, $\boldsymbol{C} = \mathrm{diag}(0.6, 0.9, 1.3)$, $\boldsymbol{A} = \mathrm{diag}(1.3, 1.0, 1.5)$, $\boldsymbol{B} = \mathrm{diag}(1.5, 0.9, 0.7)$, $\boldsymbol{G} = \mathrm{diag}(0.3, 0.5, 0.9)$. The matrices $\boldsymbol{W}, \boldsymbol{\Gamma}, \boldsymbol{Q} = (Q_{\iota i})_{6\times 6}, \boldsymbol{H} = (H_{\iota i})_{6\times 6}$ and $\boldsymbol{D}$ are selected as, respectively

$$\boldsymbol{W} = \begin{pmatrix} 0.5 & 0.2 & 0 \\ 0.1 & 0.4 & 0 \\ 0 & 0.7 & 0.3 \end{pmatrix}, \boldsymbol{\Gamma} = \begin{pmatrix} 0.6 & 0.1 & 0.2 \\ 0 & 0.4 & 0 \\ 0.2 & 0 & 0.6 \end{pmatrix}, \boldsymbol{D} = \begin{pmatrix} 0.2 & 0 & 0.4 \\ 0.5 & 0.1 & 0.6 \\ 0 & 0.3 & 0.7 \end{pmatrix},$$

$$\boldsymbol{Q} = \begin{pmatrix} -0.8 & 0 & 0.2 & 0.2 & 0.3 & 0.1 \\ 0 & -0.7 & 0.1 & 0.3 & 0.1 & 0.2 \\ 0.2 & 0.1 & -0.6 & 0.3 & 0 & 0 \\ 0.2 & 0.3 & 0.3 & -1.1 & 0.1 & 0.2 \\ 0.3 & 0.1 & 0 & 0.1 & -0.8 & 0.3 \\ 0.1 & 0.2 & 0 & 0.2 & 0.3 & -0.8 \end{pmatrix}, \boldsymbol{H} = \begin{pmatrix} -0.7 & 0.1 & 0.2 & 0 & 0.2 & 0.2 \\ 0.1 & -0.6 & 0 & 0.2 & 0.3 & 0 \\ 0.2 & 0 & -1.0 & 0.1 & 0.3 & 0.4 \\ 0 & 0.2 & 0.1 & -0.6 & 0.1 & 0.2 \\ 0.2 & 0.3 & 0.3 & 0.1 & -0.9 & 0 \\ 0.2 & 0 & 0.4 & 0.2 & 0 & -0.8 \end{pmatrix}.$$

Evidently, $f_o(\cdot)$ satisfies Assumption 1 with $\varpi_o = 0.4$. Take $T_c, \gamma_1, \boldsymbol{V} = \mathrm{diag}(0.3I_3, 0.2I_3, 0.4I_3, 0.7I_3, 0.6I_3, 0.5I_3)$ are selected as $T_c = 0.3$ and $\gamma_1 = 0.6$ such that $\gamma_1 < 1$ hold. Thus, c_1 and c_2 can be calculated as $c_1 = \frac{\pi(nM)^{\frac{\gamma_1}{2}}}{2^{\frac{2-\gamma_1}{2}}\gamma_1 T_c} = 25.5704$ and $c_2 = \frac{\pi}{2\gamma_1 T_c} = 8.7266$. The following matrix $\boldsymbol{X}$ can be obtained through programming and calculating by MATLAB

$$\boldsymbol{X} = \begin{pmatrix} 0.2998 & 0 & 0 \\ 0 & 0.3913 & 0 \\ 0 & 0 & 0.3392 \end{pmatrix},$$

which satisfies (7).

By Theorem 1, the drive-response systems (26) and (27) reach predefined-time synchronization within the predefined time $T_c = 0.3s$ under the bilayer controllers (6). When the predefined time T_c is set as $0.3s$, Figures 1 and 2 present the evolution progresses of the synchronization errors $\boldsymbol{e}_\iota(\lambda) = \boldsymbol{z}_\iota(\lambda) - \boldsymbol{y}_\iota(\lambda)$ of STM in drive-response systems (26) and (27) with and without the bilayer controllers (6). Similarly, Figures 3 and 4 respectively depict the change processes of the errors $\hat{\boldsymbol{e}}_\iota(\lambda) = \boldsymbol{\delta}_\iota(\lambda) - \boldsymbol{\theta}_\iota(\lambda)$ of LTM in drive-response systems (26) and (27) with and without the bilayer controllers (6). Obviously, all the states of the error variables $\boldsymbol{e}_\iota(\lambda)$ in Figure 1 and $\hat{\boldsymbol{e}}_\iota(\lambda)$ in Figure 3 are extremely close to 0 within the predefined time $T_c = 0.3s$, and this state is maintained along with the increase in time under the bilayer controllers (6). In contrast, Figures 2 and 4 clearly show that all error variables do not converge to zero as time increases.Thus, the drive and response systems (26) and (27) of coupled competitive NNs under consideration cannot achieve predefined-time synchronization without the implementation of the controllers. Therefore, the designed bilayer controllers (6) are effective, which also demonstrates the correctness of the result obtained in Theorem 1.

Example 5.2. Let us consider the drive and response systems of coupled competitive NNs with time-varying delays described below:

$$\begin{cases} STM: \dot{\boldsymbol{y}}_\iota(\lambda) = -\boldsymbol{C}\boldsymbol{y}_\iota(\lambda) + \boldsymbol{D}\boldsymbol{f}(\overline{\boldsymbol{y}_\iota(\lambda)}) + \boldsymbol{G}\boldsymbol{\theta}_\iota(\lambda) + 0.7\sum_{i=1}^{6} Q_{\iota i}\boldsymbol{W}\boldsymbol{y}_i(\lambda), \\ LTM: \dot{\boldsymbol{\theta}}_\iota(\lambda) = -\boldsymbol{A}\boldsymbol{\theta}_\iota(\lambda) + \boldsymbol{B}\boldsymbol{f}(\boldsymbol{y}_\iota(\lambda)) + 1.0\sum_{i=1}^{6} H_{\iota i}\boldsymbol{\Gamma}\boldsymbol{\theta}_i(\lambda), \end{cases} \tag{28}$$

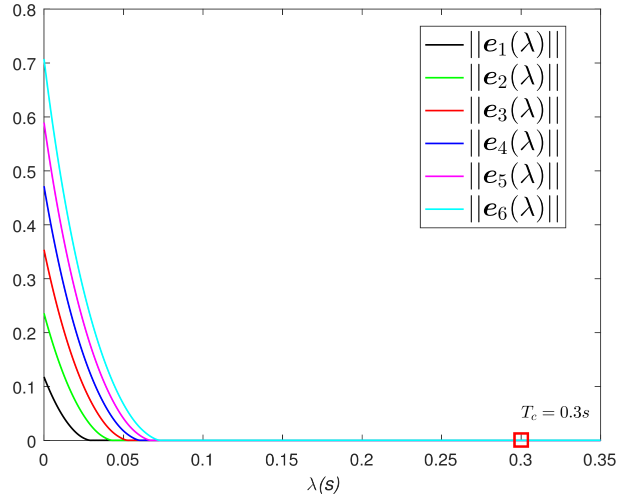

FIGURE 1 The norm of error $\boldsymbol{e}_\imath(\lambda) = \boldsymbol{z}_\imath(\lambda) - \boldsymbol{y}_\imath(\lambda)$ of STM with bilayer controllers (6) in Example 5.1, $\imath = 1, 2, \cdots, 6$.

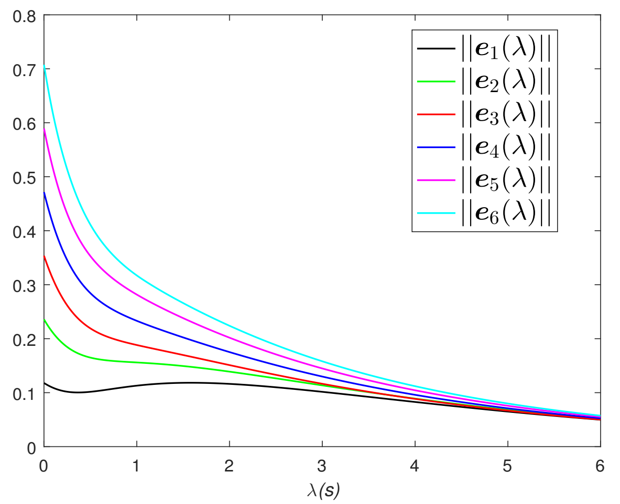

FIGURE 2 The norm of error $\boldsymbol{e}_\imath(\lambda) = \boldsymbol{z}_\imath(\lambda) - \boldsymbol{y}_\imath(\lambda)$ of STM without bilayer controllers (6) in Example 5.1, $\imath = 1, 2, \cdots, 6$.

and

$$\begin{cases} STM : \dot{\boldsymbol{z}}_\imath(\lambda) = -\boldsymbol{C}\boldsymbol{z}_\imath(\lambda) + \boldsymbol{D}\boldsymbol{f}(\overline{\boldsymbol{z}_\imath(\lambda)}) + 0.7\sum_{i=1}^{6} Q_{\imath i}\boldsymbol{W}\boldsymbol{z}_i(\lambda) + \boldsymbol{G}\boldsymbol{\delta}_\imath(\lambda) + \boldsymbol{u}_\imath(\lambda), \\ LTM : \dot{\boldsymbol{\delta}}_\imath(\lambda) = -\boldsymbol{A}\boldsymbol{\delta}_\imath(\lambda) + \boldsymbol{B}\boldsymbol{f}(\boldsymbol{z}_\imath(\lambda)) + 1.0\sum_{i=1}^{6} H_{\imath i}\boldsymbol{\Gamma}\boldsymbol{\delta}_i(\lambda) + \boldsymbol{m}_\imath(\lambda), \end{cases} \tag{29}$$

where $\imath = 1, 2, \cdots, 6$, $f_o(\phi) = \frac{|\phi+1|+|\phi-1|}{10}(o = 1, 2, 3)$, $\boldsymbol{C} = \mathrm{diag}(0.7, 1.0, 0.9)$, $\boldsymbol{A} = \mathrm{diag}(0.8, 1.1, 1.5)$, $\boldsymbol{B} = \mathrm{diag}(2.1, 1.6, 0.5)$, $\boldsymbol{G} = \mathrm{diag}(1.0, 0.6, 0.3)$. $\tau_s(\lambda) = \frac{1}{2} - \frac{1}{3+s}e^{-t}$, $\tau = \frac{1}{2}$, $\epsilon_s = \frac{1}{3+s}$, $s = 1, 2, 3$. The matrices $\boldsymbol{W}, \boldsymbol{\Gamma}, \boldsymbol{Q} = (Q_{\imath i})_{6\times 6}, \boldsymbol{H} = (H_{\imath i})_{6\times 6}$ and $\boldsymbol{D}$ are selected as, respectively

$$\boldsymbol{W} = \begin{pmatrix} 0.9 & 0.6 & 0 \\ 0 & 0.6 & 0.4 \\ 0.3 & 0.4 & 0.4 \end{pmatrix}, \boldsymbol{\Gamma} = \begin{pmatrix} 0.7 & 0 & 0.3 \\ 0.1 & 0.4 & 0 \\ 0.3 & 0 & 0.5 \end{pmatrix}, \boldsymbol{D} = \begin{pmatrix} 0.2 & 0 & 0.7 \\ 0.4 & 0.1 & 0.6 \\ 0.2 & 0 & 0.8 \end{pmatrix},$$

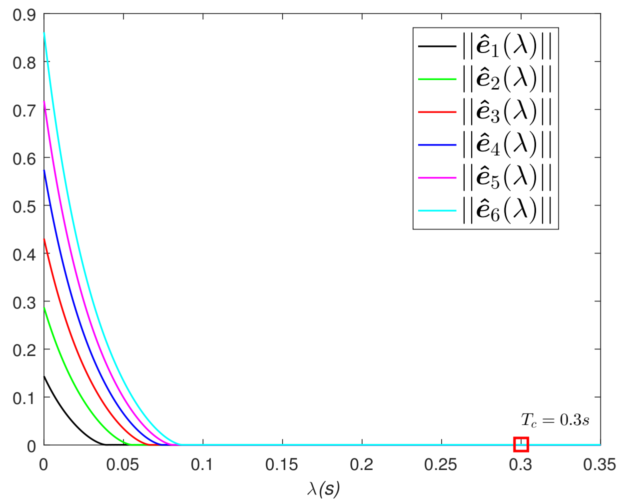

FIGURE 3 The norm of error $\hat{\boldsymbol{e}}_\iota(\lambda) = \boldsymbol{\delta}_\iota(\lambda) - \boldsymbol{\theta}_\iota(\lambda)$ of LTM with bilayer controllers (6) in Example 5.1, $\iota = 1, 2, \cdots, 6$.

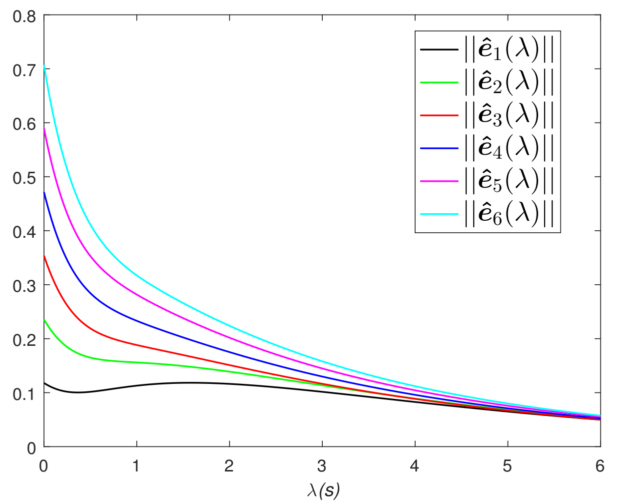

FIGURE 4 The norm of error $\hat{\boldsymbol{e}}_\iota(\lambda) = \boldsymbol{\delta}_\iota(\lambda) - \boldsymbol{\theta}_\iota(\lambda)$ of LTM without bilayer controllers (6) in Example 5.1, $\iota = 1, 2, \cdots, 6$.

$$\boldsymbol{Q} = \begin{pmatrix} -0.9 & 0.1 & 0 & 0.3 & 0.4 & 0.1 \\ 0.1 & -0.8 & 0.2 & 0.1 & 0.2 & 0.2 \\ 0 & 0.2 & -1.1 & 0.3 & 0.3 & 0.3 \\ 0.3 & 0.1 & 0.3 & -0.8 & 0 & 0.1 \\ 0.4 & 0.2 & 0.3 & 0 & -1.2 & 0.3 \\ 0.1 & 0.2 & 0.3 & 0.1 & 0.3 & -1.0 \end{pmatrix}, \boldsymbol{H} = \begin{pmatrix} -0.6 & 0.2 & 0.1 & 0.1 & 0.1 & 0.1 \\ 0.2 & -0.9 & 0.2 & 0.2 & 0 & 0.3 \\ 0.1 & 0.2 & -0.9 & 0.3 & 0 & 0.3 \\ 0.1 & 0.2 & 0.3 & -1.0 & 0.2 & 0.2 \\ 0.1 & 0 & 0 & 0.2 & -0.7 & 0.4 \\ 0.1 & 0.3 & 0.3 & 0.2 & 0.4 & -1.3 \end{pmatrix}.$$

Evidently, $f_o(\cdot)$ satisfies Assumption 1 with $\varpi_o = 0.2$. Take T_c, γ_1, $\boldsymbol{V} = \mathrm{diag}(0.6I_3, 0.3I_3, 0.5I_3, 0.7I_3, 0.4I_3, 0.6I_3)$ are selected as $T_c = 1.2$ and $\gamma_1 = 0.4$ such that $\gamma_1 < 1$ hold. Hence, c_1 and c_2 can be calculated as $c_1 = \frac{\pi(nM)^{\frac{\gamma_1}{2}}}{2^{1-\gamma_1}\gamma_1 T_c} = 7.6974$ and $c_2 = \frac{\pi}{2\gamma_1 T_c} = 3.2725$. The following matrix $\boldsymbol{X}$ can be obtained through programming and calculating by MATLAB

$$\boldsymbol{X} = \begin{pmatrix} 0.2260 & 0 & 0 \\ 0 & 0.2528 & 0 \\ 0 & 0 & 0.2469 \end{pmatrix},$$

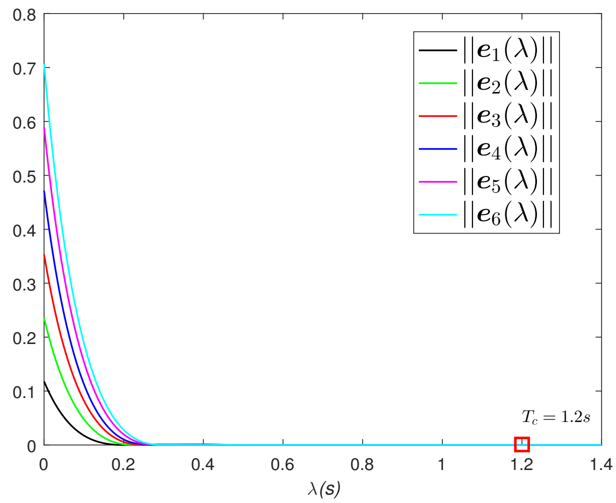

FIGURE 5 The norm of error $\boldsymbol{e}_\imath(\lambda) = \boldsymbol{z}_\imath(\lambda) - \boldsymbol{y}_\imath(\lambda)$ of STM with bilayer controllers (20) in Example 5.2, $\imath = 1, 2, \cdots, 6$.

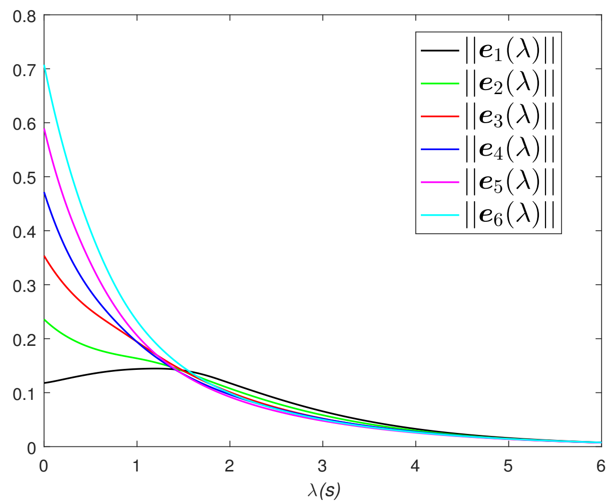

FIGURE 6 The norm of error $\boldsymbol{e}_\imath(\lambda) = \boldsymbol{z}_\imath(\lambda) - \boldsymbol{y}_\imath(\lambda)$ of STM without bilayer controllers (20) in Example 5.2, $\imath = 1, 2, \cdots, 6$.

which satisfies (21).

According to Theorem 2, the drive-response systems (28) and (29) achieve predefined-time synchronization within the predefined time $T_c = 1.2s$ under the implementation of the bilayer controllers (20). The norms of the synchronization errors $\boldsymbol{e}_\imath(\lambda) = \boldsymbol{z}_\imath(\lambda) - \boldsymbol{y}_\imath(\lambda)$ of STM in drive-response systems (28) and (29) with and without the bilayer controllers (20) are revealed respectively in Figures 5 and 6. In the same way, the varying processes of errors $\hat{\boldsymbol{e}}_\imath(\lambda) = \boldsymbol{\delta}_\imath(\lambda) - \boldsymbol{\theta}_\imath(\lambda)$ of LTM in drive-response systems (28) and (29) with and without the bilayer controllers (20) are showed as in Figures 7 and 8. When the predefined time T_c is set as $1.2s$, it is easy to see that all the states of error variables $\boldsymbol{e}_\imath(\lambda)$ in Figure 5 and $\hat{\boldsymbol{e}}_\imath(\lambda)$ in Figure 7 converge to 0 within the predefined time $T_c = 1.2s$ under the action of the bilayer controllers (20). However, without the action of the controllers (20), all the states of the error variables in Figures 6 and 8 cannot converge to zero before the predefined time $T_c = 1.2s$. Consequently, the drive and response systems (28) and (29) of coupled competitive NNs cannot achieve synchronization within the predefined-time when the bilayer controllers (20) are not implemented, which demonstrates the validness of the designed controllers (20) and the accuracy of the obtained result in Theorem 2.

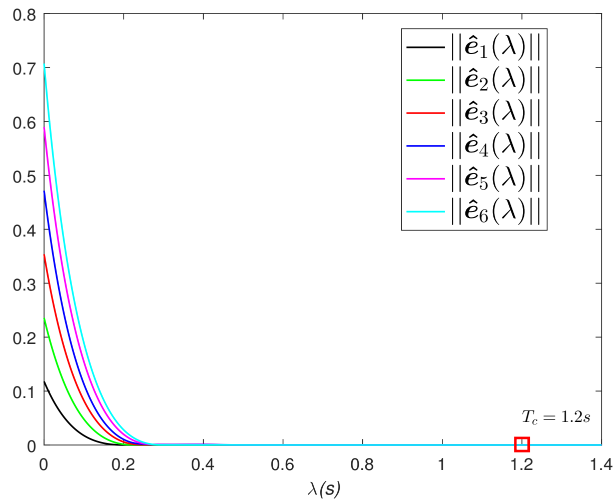

FIGURE 7 The norm of error $\hat{\boldsymbol{e}}_\imath(\lambda) = \boldsymbol{\delta}_\imath(\lambda) - \boldsymbol{\theta}_\imath(\lambda)$ of LTM with bilayer controllers (20) in Example 5.2, $\imath = 1, 2, \cdots, 6$.

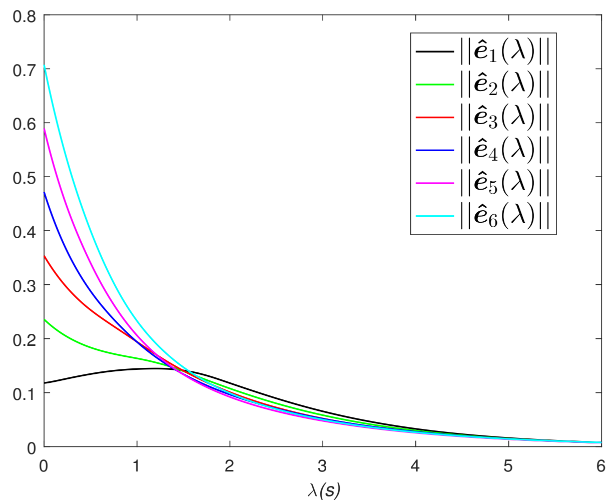

FIGURE 8 The norm of error $\hat{\boldsymbol{e}}_\imath(\lambda) = \boldsymbol{\delta}_\imath(\lambda) - \boldsymbol{\theta}_\imath(\lambda)$ of LTM without bilayer controllers (20) in Example 5.2, $\imath = 1, 2, \cdots, 6$.

Remark 6. In most cases, the drive-response systems of coupled competitive NNs could not achieve predefined-time synchronization themselves. Therefore, it is necessary to adopt suitable control strategies to realize synchronization in the predefined time for the considered network. As previously mentioned in Examples 5.1 and 5.2 and displayed in Figures 2, 4, 6 and 8, the drive-response systems of coupled competitive NNs without and with time-varying delays cannot achieve predefined-time synchronization without the action of the controllers (6) and (20). Thus, it is extremely important to design appropriate controllers for achieving predefined-time synchronization of the considered coupled competitive NNs. In this paper, by designing novel bilayer controllers, two sufficient predefined-time synchronization conditions are established respectively for coupled competitive NNs without and with time-varying delays. To the authors' knowledge, this is the first investigation on the synchronization of coupled competitive NNs in predefined time.

6 | CONCLUSION

In this paper, two types of coupled competitive NNs without and with time-varying delays have been examined. Firstly, a sufficient predefined-time synchronization condition has been obtained for the considered coupled competitive NNs based on the some inequality theories and the proposed bilayer controllers. Moreover, time-varying delays are also considered in the given network model, by constructing new applicable Lyapunov functional and designing new appropriate controllers, another criterion has been presented to enable coupled competitive NNs with time-varying delays in achieving predefined-time synchronization. Finally, the effectiveness of the proposed approach has been proved through the demonstration of two numerical examples. As a good candidate for the synapse, memristor is a novel type of nonlinear resistor with memory properties, which can be applied in NNs to better simulate human brains. Recently, the memristor-based competitive NNs have been studied by more and more scholars [12, 13, 17]. Therefore, it would be very interesting to incorporate memristive property into coupled competitive NNs and study predefined-time synchronization of memristor-based coupled competitive NNs in the near future. Moreover, it is known to all that fractional calculus is a theory that generalizes the concept of calculus from the integer order to arbitrary order [1, 3, 13, 14]. For example, the authors investigated global Mittag-Leffler stability of fractional-order quaternion-valued memristive neural networks in [3]. Motivated by these works, it would be also a very interesting problem of research to consider the fractional operators in coupled competitive NNs and study predefined-time synchronization of this kind of fractional-order network model.

ACKNOWLEDGMENTS

The authors would like to thank the Editor and anonymous reviewers for their valuable comments and suggestions for improving this manuscript. This work was supported by the National Natural Science Foundation of China under Grants 62173244 and 62173016.

References

[1] G. Rajchakit, A. Pratap, R. Raja, J. Cao, J. Alzabut, C. Huang. Hybrid control scheme for projective lag synchronization of Riemann-Liouville sense fractional order memristive BAM neural networks with mixed delays. Mathematics 2019; 7: 759. https://doi.org/10.3390/math7080759.

[2] G. Rajchakit, R. Sriraman. Robust passivity and stability analysis of uncertain complex-valued impulsive neural networks with time-varying delays. Neural Processing Letters 2021; 53: 581–606. https://doi.org/10.1007/s11063-020-10401-w.

[3] G. Rajchakit, P. Chanthorn, P. Kaewmesri, R. Sriraman, C. P. Lim. Global Mittag-Leffler stability and stabilization analysis of fractional-order quaternion-valued memristive neural networks. Mathematics 2020; 8: 422. https://doi.org/10.3390/math8030422.

[4] G. Rajchakit, R. Sriraman, N. Boonsatit, P. Hammachukiattikul, C. P. Lim, P. Agarwal. Global exponential stability of Clifford-valued neural networks with time-varying delays and impulsive effects. Advances in Difference Equations 2021; 2021: 208. https://doi.org/10.1186/s13662-021-03367-z.

[5] G. Rajchakit, P. Agarwal, R. Sriraman. Stability analysis of neural networks. Springer eBooks 2021; https://doi.org/10.1007/978-981-16-6534-9.

[6] J. Xiao, Y. Hu, Z. Zeng, A. Wu, S. Wen. Fixed/predefined-time synchronization of memristive neural networks based on state variable index coefficient. Neurocomputing 2023; 560:126849. https://doi.org/10.1016/j.neucom.2023.126849.

[7] W. Zhou, Y. Hu, X. Liu, J. Cao. Finite-time adaptive synchronization of coupled uncertain neural networks via intermittent control. Physica A: Statistical Mechanics and its Applications 2022; 596: 127107. https://doi.org/10.1016/j.physa.2022.127107.

[8] M. A. Cohen, S. Grossberg. Absolute stability of global pattern formation and parallel memory storage by competitive neural networks. IEEE transactions on systems, man, and cybernetics 1983; 5: 815–826. https://doi.org/10.1016/S0166-4115(08)60913-9.

[9] A. Meyer-Bäse, F. Ohl, H. Scheich. Singular perturbation analysis of competitive neural networks with different time scales. Neural Computation 1996; 8: 1731–1742. https://doi.org/10.1162/neco.1996.8.8.1731.

[10] E. Araujo, G. E. Bentes, R. Zangaro. Body sway and global equilibrium condition of the elderly in quiet standing posture by using competitive neural networks. Applied Soft Computing 2018; 69: 625–633. https://doi.org/10.1016/j.asoc.2018.05.004.

[11] Z. Shi, Y. Yang, Q. Chang, X. Xu. The optimal state estimation for competitive neural network with time-varying delay using local search algorithm. Physica A: Statistical Mechanics and its Applications 2020; 540: 123102. https://doi.org/10.1016/j.physa.2019.123102.

[12] Y. Zhao, S. Ren, J. Kurths. Finite-time and fixed-time synchronization for a class of memristor-based competitive neural networks with different time scales. Chaos, Solitons & Fractals 2021; 148: 111033. https://doi.org/10.1016/j.chaos.2021.111033.

[13] G. Rajchakit, P. Chanthorn, M. Niezabitowski, R. Raja, D. Baleanu, A. Pratap. Impulsive effects on stability and passivity analysis of memristor-based fractional-order competitive neural networks. Neurocomputing 2020; 417: 290–301. https://doi.org/10.1016/j.neucom.2020.07.036.

[14] S. Yang, H. Jiang, C. Hu, J. Yu. Synchronization for fractional-order reaction–diffusion competitive neural networks with leakage and discrete delays. Neurocomputing 2021; 436: 47–57. https://doi.org/10.1016/j.neucom.2021.01.009.

[15] Y. Zou, H. Su, R. Tang, X. Yang. Finite-time bipartite synchronization of switched competitive neural networks with time delay via quantized control. ISA transactions 2022; 125: 156–165. https://doi.org/10.1016/j.isatra.2021.06.015.

[16] C. Zheng, C. Hu, J. Yu, H. Jiang. Fixed-time synchronization of discontinuous competitive neural networks with time-varying delays. Neural Networks 2022; 153: 192–203. https://doi.org/10.1016/j.neunet.2022.06.002.

[17] Y. Zhao, S. Ren, J. Kurths. Synchronization of coupled memristive competitive bam neural networks with different time scales. Neurocomputing 2021; 427: 110–117. https://doi.org/10.1016/j.neucom.2020.11.023.

[18] Y. Zou, X. Yang, R. Tang, Z. Cheng. Finite-time quantized synchronization of coupled discontinuous competitive neural networks with proportional delay and impulsive effects. Journal of the Franklin Institute 2020; 357(16): 11136–11152. https://doi.org/10.1016/j.jfranklin.2019.05.017.

[19] G. Kamenkov. On stability of motion over a finite interval of time. Journal of Applied Mathematics and Mechanics 1953; 17(2): 529–540.

[20] I. Ahmad, M. Shafiq, M. Shahzad. Global finite-time multi-switching synchronization of externally perturbed chaotic oscillators. Circuits Systems and Signal Processing 2018; 37(12): 5253–5278. https://doi.org/10.1007/s00034-018-0826-4.

[21] I. Ahmad, M. Shafiq. A generalized analytical approach for the synchronization of multiple chaotic systems in the finite time. Arabian Journal for Science and Engineering 2020; 45(3): 2297–2315. https://doi.org/10.1007/s13369-019-04304-9.

[22] Y. Li, X. Yang, L. Shi. Finite-time synchronization for competitive neural networks with mixed delays and non-identical perturbations. Neurocomputing 2016; 185: 242–253. https://doi.org/10.1016/j.neucom.2015.11.094.

[23] C. Aouiti, E. A. Assali, F. Chérif, A. Zeglaoui. Fixed-time synchronization of competitive neural networks with proportional delays and impulsive effect. Neural Computing and Applications 2020; 32: 13245–13254. https://doi.org/10.1007/s00521-019-04654-3.

[24] J. D. Sánchez-Torres, E. N. Sanchez, A. G. Loukianov. Predefined-time stability of dynamical systems with sliding modes. 2015 IEEE American control conference (ACC) 2015: 5842–5846. https://doi.org/10.1109/ACC.2015.7172255.

[25] Y. Wang, H. Li, Y. Guan, M. Chen. Predefined-time chaos synchronization of memristor chaotic systems by using simplified control inputs. Chaos, Solitons & Fractals 2022; 161: 112282. https://doi.org/10.1016/j.chaos.2022.112282.

[26] C. Chen, L. Mi, Z. Liu, B. Qiu, H. Zhao, L. Xu. Predefined-time synchronization of competitive neural networks. Neural Networks 2021; 142: 492–499. https://doi.org/10.1016/j.neunet.2021.06.026.

[27] A. Liu, H. Zhao, Q. Wang, S. Niu, X. Gao, C. Chen, L. Li. A new predefined-time stability theorem and its application in the synchronization of memristive complex-valued bam neural networks. Neural Networks 2022; 153: 152–163. https://doi.org/10.1016/j.neunet.2022.05.031.

[28] C. A. Anguiano-Gijón, A. J. Muñoz-Vázquez, J. D. Sánchez-Torres, G. Romero-Galván, F. Martínez-Reyes. On predefined-time synchronisation of chaotic systems. Chaos, Solitons & Fractals 2019; 122: 172–178. https://doi.org/10.1016/j.chaos.2019.03.015.